

## Supplementary Information

### Targeting the APP-Mint2 protein-protein interaction with a peptide based-inhibitor reduces amyloid- $\beta$ formation

Christian R. O. Bartling,<sup>†,‡,⊥</sup> Thomas M. T. Jensen,<sup>†,⊥</sup> Shawna M. Henry,<sup>‡,⊥</sup> Anna L. Colliander,<sup>†</sup> Vita Sereikaite,<sup>†</sup> Marcella Wenzler,<sup>†</sup> Palash Jain,<sup>†</sup> Hans M. Maric,<sup>†,§</sup> Kasper Harpsøe,<sup>†</sup> Søren W. Pedersen,<sup>†</sup> Louise S. Clemmensen,<sup>†</sup> Linda M. Haugaard-Kedström,<sup>†</sup> David E. Gloriam,<sup>†</sup> Angela Ho,<sup>‡</sup> and Kristian Strømgaard<sup>\*,†</sup>

<sup>†</sup> Department of Drug Design and Pharmacology, University of Copenhagen, Jagtvej 162, DK-2100 Copenhagen, Denmark.

<sup>‡</sup> Department of Biology, Boston University, 24 Cummington Mall, Boston, MA 02215, USA.

<sup>§</sup> Rudolf Virchow Center for Experimental Biomedicine, University of Würzburg, Josef-Schneider-Str. 2, 97080 Würzburg, Germany; formerly Department of Drug Design and Pharmacology, University of Copenhagen, Universitetsparken 2, 2100 Copenhagen, Denmark; Department of Biotechnology and Biophysics, Biocenter, University of Würzburg, Am Hubland, 97074 Würzburg, Germany.

<sup>⊥</sup> Shared first authors

\* To whom correspondence should be addressed  
e-mail: [kristian.stromgaard@sund.ku.dk](mailto:kristian.stromgaard@sund.ku.dk)

## Table of Contents

Supplemental Methods.....	3
Detailed Methods.....	9
Figure S1. The affinity of the human 17-mer APP peptide.....	22
Figure S2. Binding data and comparison of secondary structure of Mint2-PARM variants.....	23
Figure S3. Binding data and comparison of secondary structure of expressed Mint2-PARM and Mint2-pPARM <sub>SS</sub> .....	24
Figure S4. Synthesis of depsipeptide fragment $\Delta$ pepPARM (A453-S478) and secondary structure of Mint2-pPARM <sub>SS</sub> A-to-E variant.....	25
Figure S5. Characterization of Mint2-pPARM <sub>SS</sub> A to-E variants by UPLC and LC-MS.....	26
Figure S6. SDS-PAGE of Mint2-pPARM <sub>SS</sub> A-to-E variants.....	28
Figure S7. Effect of A-to-E substitutions on the melting temperature ( $T_m$ ) of pPARM <sub>SS</sub> variants. ....	29
Figure S8. Binding affinities of Ala, A-to-E, D-AA and NMe-AA variants of APP <sub>WT</sub> . ....	30
Figure S9. Binding and secondary structure characterization of Mint2-PARM Ala and Mint2-pPARM <sub>SS</sub> A-to-E variants. ....	31
Figure S10. Mutational scan of L454, Y459 and F520 in Mint2-PARM ....	32
Figure S11. Sequence alignment of Mint proteins ....	33
Figure S12. Synthesis, structural feasibility, binding affinity and metabolic stability of cyclic APP <sub>WT</sub> variants ....	35
Figure S13. Representative ITC spectra of KSL-221036 (14, a) and the APP <sub>WT</sub> peptide (b) ....	36
Figure S14. Pull down of full length Mint2 using coated bead containing KSL-221036 (14) and APP <sub>WT</sub> ....	37
Figure S15. Cytotoxicity of peptides. ....	38
Figure S16. A $\beta$ <sub>42</sub> ELISA data and corresponding LDH data for each individual experiment.....	39
Figure S17. Representative images of TAT-immunostaining.....	40
Table S1. Characterization and affinities of APP peptides ....	41
Table S2. Characterization and affinities of PARM variants. ....	44
Table S3. Characterization of PARM peptide fragments.....	44
Table S4. Characterization of semi synthetic Mint2-pPARM <sub>SS</sub> A-to-E variants and APP <sub>WT</sub> affinity.....	45
Supplementary References:.....	46

## Supplemental Methods:

### Synthesis and characterization of $\alpha$ -hydroxy acids and ester building blocks

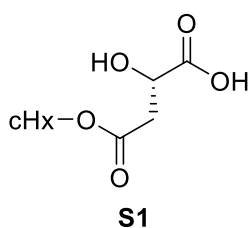
**General information:** All starting materials were purchased from commercial sources and used without further purification. Solvents were dried under standard conditions. Reactions were monitored by thin-layer chromatography (TLC) using silica gel coated aluminum plates 60F-254 (Merck). A CombiFlashR<sub>f</sub><sup>TM</sup> system (Teledyne ISCO) was used for flash column chromatography with samples being loaded onto GraceResolv<sup>TM</sup> flash cartridges (Grace). NMR spectroscopy was performed on a Bruker 400 MHz apparatus and CDCl<sub>3</sub> was used as solvent unless otherwise stated. <sup>1</sup>H NMR chemical shifts were recorded in ppm using tetramethylsilane (TMS) as internal standard (0.0 ppm). The following abbreviations are used: s, singlet; d, doublet; t, triplet; q, quartet; m, multiplet; br s, broad singlet; dd, doublet of doublets; dt, doublet of triplets; dq, doublet of quartets; qd, quartet of doublets; ddt, doublet of doublet of triplets. <sup>13</sup>C NMR shifts are recorded in ppm using the residual non deuterated solvent as internal standard (CDCl<sub>3</sub> <sup>13</sup>C, 77.0 ppm). Analysis of all NMR spectra was performed with MestReNova version 10.0.2 (Mestrec Laboratories). Mass spectra were obtained with an Agilent 6410 Triple Quadrupole Mass Spectrometer instrument using electron spray ionisation coupled to an Agilent 1200 HPLC system (ESI-LC/MS) with a C18 reverse phase column (Zorbax Eclipse XBD-C18, 4.6 × 50 mm), autosampler and diode-array detector using a linear gradient of the binary solvent system of H<sub>2</sub>O/MeCN/formic acid (buffer A: 95/5/0.1 and buffer B: 5/95/0.01) with a flow rate of 1 mL/min, and gradient elution from 0-100% buffer B in 5 min.

**General procedure A. Conversion of amino acids to  $\alpha$ -hydroxy acids:**<sup>1-3</sup> The amino acid (AA) (1 eq) was dissolved in a mixture of dioxane/H<sub>2</sub>O (1:1 v/v, 2 mL) and TFA (0.5 mL) and the mixture was placed under nitrogen and stirred at 0 °C, followed by addition of *tert*-butylnitrite (2 eq). The reaction mixture was stirred at room temperature (RT) for 24 h. Upon completion, the solvent was removed *in vacuo* and the resulting residue was purified by silica gel chromatography (DCM/MeOH 10:1 unless otherwise stated) to afford the  $\alpha$ -hydroxy acid.

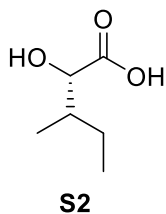
**General procedure B. Ester bond formation:**<sup>4</sup> *O*-Protected  $\alpha$ -hydroxy acid (1 eq) and Boc protected AA (1.2 eq) were dissolved in DCM (1.5 mL), followed by addition of dicyclohexylcarbodiimide (DCC, 1.2 eq) and 4-dimethylaminopyridine (DMAP, 0.2 eq) and the resulting mixture was stirred for 2 h at RT. Upon completion, the reaction mixture was filtered and

excess DCM was removed *in vacuo*. The residue was purified by silica gel chromatography (heptane/EtOAc 3:2) to afford the desired *O*-protected ester building block (BB).

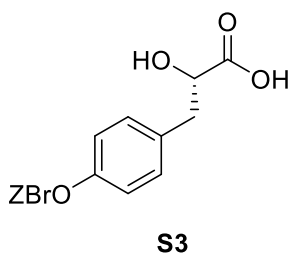
**General procedure C. Allyl deprotection:**<sup>5</sup> *O*-Protected ester BB (1 eq) and Pd(PPh<sub>3</sub>)<sub>4</sub> (0.1 eq) were dissolved in dry THF (10 mL) and the reaction was mixture stirred under nitrogen for 5 min, followed by addition of morpholine (10 eq) and subsequently stirring for 20 min at RT. The solvent was removed *in vacuo* and the resulting residue was dissolved in DCM (10 mL), washed with 1M HCl (2 × 5 mL), dried (MgSO<sub>4</sub>) and excess solvent was removed *in vacuo*. The crude product was purified by silica gel chromatography (DCM/MeOH 10:1) to afford the desired ester BB.



**(S)-4-(Cyclohexyloxy)-2-hydroxy-4-oxobutanoic acid (S1)** was synthesized according to *General procedure A*, using H-Asp(cHx)-OH (2.15 g, 10 mmol). **S1** was obtained as yellowish oil (822 mg, 38%). <sup>1</sup>H NMR (400 MHz, CDCl<sub>3</sub>) δ 4.88-4.77 (m, 1H), 4.54 (dd, *J* = 6.1, 4.8 Hz, 1H), 2.95-2.80 (m, 2H), 1.90-1.67 (m, 4H), 1.57-1.24 (m, 6H). <sup>13</sup>C NMR (100 MHz, CDCl<sub>3</sub>) δ 176.4, 171.0, 74.4, 67.2, 38.6, 31.6, 25.4, 23.8.

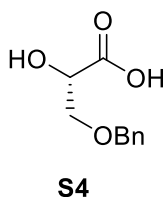


**(2S,3R)-2-Hydroxy-3-methylpentanoic acid (S2)** was synthesized according to *General procedure A*, using H-Ile-OH (1.31 g, 10 mmol). **S2** was obtained as white solid (660 mg, 50%). <sup>1</sup>H NMR (400 MHz, CDCl<sub>3</sub>) δ 4.18 (d, *J* = 3.7 Hz, 1H), 1.96-1.83 (m, 1H), 1.50-1.23 (m, 2H), 1.03 (d, *J* = 6.9 Hz, 3H), 0.93 (t, *J* = 7.4 Hz, 3H). <sup>13</sup>C NMR (100 MHz, CDCl<sub>3</sub>) δ 179.6, 74.8, 39.1, 23.8, 15.5, 11.9.

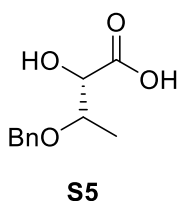


**(S)-3-(4-(((2-Bromobenzyl) oxy) carbonyl) oxy) phenyl)-2-hydroxypropanoic acid (S3)**. Boc-Tyr(BrZ)-OH (1.48 g, 3 mmol) was treated with TFA (9 mL) for 20 min at RT to obtain *N*-unprotected product. After evaporation the residue was used for synthesis of **S3** according to *General procedure A*. **S3** was obtained as yellowish solid (830 mg, 70%). <sup>1</sup>H NMR (400 MHz, CDCl<sub>3</sub>) δ 7.61 (dd, *J* = 7.9, 1.3 Hz, 1H), 7.50 (dd, *J* = 7.7, 1.7 Hz, 1H), 7.35 (td, *J* = 7.5, 1.3 Hz, 1H), 7.30-7.26 (m, 2H), 7.23 (td, *J* = 7.7, 1.8 Hz, 1H), 7.18-7.10 (m, 2H), 5.36 (s, 2H), 4.49 (dd, *J* = 7.2, 4.1 Hz, 1H), 3.23-2.95 (m, 2H). <sup>13</sup>C NMR (100 MHz, CDCl<sub>3</sub>) δ 177.5, 153.7,

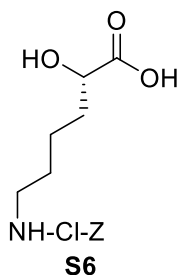
150.3, 134.3, 134.2, 133.1, 130.8, 130.4, 130.3, 127.8, 123.6, 121.2, 121.1, 71.0, 69.9, 39.6.



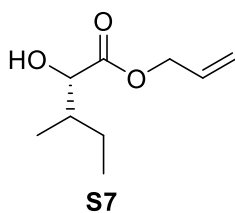
**(S)-3-(Benzyloxy)-2-hydroxypropanoic acid (S4)** was synthesized according to *General procedure A*, using H-Ser(Bn)-OH (1.95 g, 10 mmol). **S4** was obtained as colorless oil (1.08 g, 55%).  $^1\text{H}$  NMR (400 MHz,  $\text{CDCl}_3$ )  $\delta$  7.37-7.26 (m, 5H), 4.65-4.52 (m, 2H), 4.37 (t,  $J = 4.1$  Hz, 1H), 3.84-3.73 (m, 2H).  $^{13}\text{C}$  NMR (100 MHz,  $\text{CDCl}_3$ )  $\delta$  175.7, 137.2, 128.7 (2C), 128.2, 128.0 (2C), 73.9, 70.9, 70.3.



**(2S,3R)-3-(Benzyloxy)-2-hydroxybutanoic acid (S5)**. Boc-Thr(Bn)-OH (928 mg, 3 mmol) was treated with TFA (9 mL) for 20 min at RT to obtain *N*-unprotected product. After evaporation the residue was used for synthesis of **S5** according to *General procedure A*. **S5** was obtained as white solid (454 mg, 72%).  $^1\text{H}$  NMR (400 MHz,  $\text{CDCl}_3$ )  $\delta$  7.37-7.26 (m, 5H), 4.70-4.46 (m, 2H), 4.16 (d,  $J = 3.4$  Hz, 1H), 4.02 (qd,  $J = 6.4, 3.3$  Hz, 1H), 1.31 (d,  $J = 6.4$  Hz, 3H).  $^{13}\text{C}$  NMR (100 MHz,  $\text{CDCl}_3$ )  $\delta$  175.5, 137.2, 128.7 (2C), 128.3, 128.0 (2C), 74.8, 73.2, 71.6, 15.3.

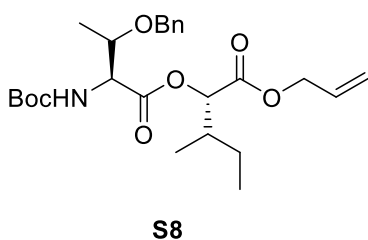


**(S)-6-(((2-Chlorobenzyl)oxy)carbonyl)amino)-2-hydroxyhexanoic acid (S6)** was synthesized according to *General procedure A*, using H-Lys(Cl-Z)-OH (944 mg, 3 mmol). **S6** was obtained as yellowish solid (455 mg, 48%).  $^1\text{H}$  NMR (400 MHz,  $\text{CDCl}_3$ )  $\delta$  7.45-7.34 (m, 2H), 7.28 (d,  $J = 3.8$  Hz, 1H), 7.25 (d,  $J = 5.9$  Hz, 1H), 5.23 (d,  $J = 19.2$  Hz, 2H), 4.26 (d,  $J = 7.3$  Hz, 1H), 3.21 (q,  $J = 6.4$  Hz, 2H), 1.95-1.64 (m, 2H), 1.51 (ddd,  $J = 19.8, 15.4, 8.9$  Hz, 4H).  $^{13}\text{C}$  NMR (100 MHz,  $\text{CDCl}_3$ )  $\delta$  178.0, 156.8, 138.3, 133.7, 129.9, 129.7, 129.6, 127.0, 70.2, 64.3, 40.8, 33.5, 29.6, 21.9.

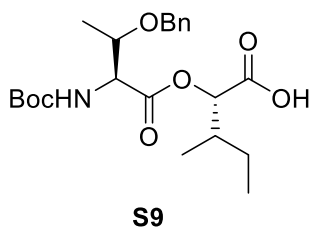


**Allyl (2S,3R)-2-hydroxy-3-methylpentanoate (S7)**. **S2** (783 mg, 5.92 mmol) was dissolved in acetone (20 mL) and  $\text{K}_2\text{CO}_3$  (1.23 g, 8.8 mmol) was added, followed by slow addition of allylbromide (1.02 mL, 11.84 mmol). The reaction mixture was stirred for 17 h at

RT. The solvent was evaporated *in vacuo* and the residue was redissolved in EtOAc (20 mL), washed with 5% NaHCO<sub>3</sub> (2 × 15 mL) and brine (40 mL), dried (MgSO<sub>4</sub>) and concentrated *in vacuo*. Allyl ester **S7** was obtained as colorless oil (510 mg, 50%). <sup>1</sup>H NMR (400 MHz, CDCl<sub>3</sub>) δ 5.93 (ddt, *J* = 17.2, 10.4, 5.9 Hz, 1H), 5.40-5.23 (m, 2H), 4.74-4.58 (m, 2H), 4.11 (dd, *J* = 6.1, 3.7 Hz, 1H), 2.69 (d, *J* = 6.1 Hz, 1H), 1.90-1.77 (m, 1H), 1.41-1.22 (m, 2H), 0.99 (d, *J* = 6.9 Hz, 3H), 0.90 (t, *J* = 7.4 Hz, 3H). <sup>13</sup>C NMR (100 MHz, CDCl<sub>3</sub>) δ 174.9, 131.6, 119.3, 75.0, 66.2, 39.3, 23.9, 15.6, 11.9.

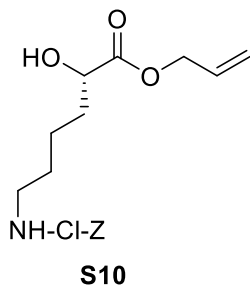


**Allyl (2S,3R)-2-((O-benzyl-N-(tert-butoxycarbonyl)-L-allothroonyloxy)-3-methylpentanoate (S8)** was synthesized according *General procedure B* using **S7** (507 mg, 3.84 mmol) and Boc-Thr(OBn)-OH (1.13 g, 4.62 mmol). **S8** was obtained as a colorless oil (1.41 g, 79%). <sup>1</sup>H NMR (400 MHz, CDCl<sub>3</sub>) δ 7.34-7.26 (m, 4H), 7.26-7.18 (m, 1H), 5.86 (ddt, *J* = 17.2, 10.4, 5.9 Hz, 1H), 5.34 – 5.29 (m, 1H), 5.27-5.18 (m, 1H), 5.02 (d, *J* = 4.6 Hz, 1H), 4.63-4.51 (m, 4H), 4.38-4.32 (m, 1H), 4.26 (qdt, *J* = 6.3, 2.1 Hz, 1H), 2.01 (dq, *J* = 9.1, 6.9, 4.6 Hz, 1H), 1.44 (d, *J* = 2.0 Hz, 9H), 1.29 (dd, *J* = 6.4, 3.2 Hz, 5H), 0.99-0.89 (m, 6H). <sup>13</sup>C NMR (100 MHz, CDCl<sub>3</sub>) δ 171.1, 169.1, 156.3, 138.5, 131.7, 128.7, 128.5, 128.4, 127.9, 127.7, 119.0, 80.0, 75.1, 71.5, 65.8, 58.2, 37.0, 28.5, 24.8, 17.1, 15.4, 11.7.

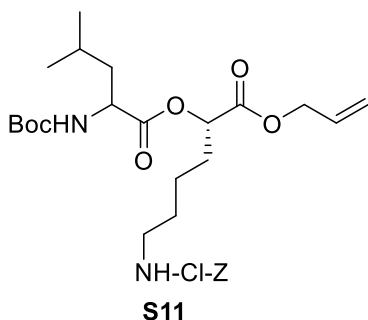


**(2S,3R)-2-((O-benzyl-N-(tert-butoxycarbonyl)-L-allothroonyloxy)-3-methylpentanoic acid (S9)** was synthesized according *General procedure C* using **S8** (463 mg, 1.0 mmol) and **S9** was obtained as a yellowish solid (263 mg, 62%). <sup>1</sup>H NMR (400 MHz, CDCl<sub>3</sub>) δ 7.30 (dddd, *J* = 12.0, 7.4, 4.6, 1.6 Hz, 4H), 7.26-7.21 (m, 1H), 5.34 (d, *J* = 8.9 Hz, 1H), 4.52-4.40 (m, 2H), 4.34 (dd, *J* = 9.0, 2.4 Hz, 1H), 4.21 (qd, *J* = 6.4, 2.2 Hz, 1H), 2.07-1.97 (m, 1H), 1.50 (dtd, *J* = 13.8, 7.4, 4.6 Hz, 1H), 1.44 (d, *J* = 2.8 Hz, 9H), 1.28 (s, 4H), 1.00-0.86 (m, 6H). <sup>13</sup>C NMR (100 MHz, CDCl<sub>3</sub>) δ 172.8,

170.5, 156.7, 137.9, 128.5, 127.9, 80.6, 74.7, 71.5, 58.2, 37.0, 28.5, 24.5, 16.8, 15.3, 11.7.

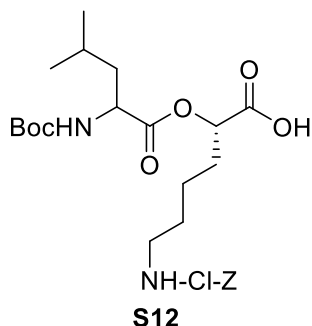


**Allyl (S)-6-((((2-chlorobenzyl)oxy)carbonyl)amino)-2-hydroxyhexanoate (S10).** **S6** (410 mg, 1.3 mmol) was dissolved in DMF (3 mL) and Cs<sub>2</sub>CO<sub>3</sub> (847 mg, 2.6 mmol) was added to reaction mixture, followed by slow addition of allylbromide (0.281 mL, 3.25 mmol). The reaction mixture was stirred for 3 h at RT. The mixture was diluted with H<sub>2</sub>O (6 mL). The aqueous layer was extracted with EtOAc (3 × 10 mL), the combined organic phases were washed with brine (20 mL), dried (MgSO<sub>4</sub>) and excess solvent removed *in vacuo*. The crude product was purified by silica gel chromatography (heptane/EtOAc 3:2). **S10** was obtained as a colorless oil (285 mg, 61%). <sup>1</sup>H NMR (400 MHz, CDCl<sub>3</sub>) δ 7.45-7.34 (m, 2H), 7.32-7.26 (m, 1H), 7.25 (d, *J* = 2.8 Hz, 1H), 5.92 (ddt, *J* = 17.2, 10.4, 5.9 Hz, 1H), 5.34 (dq, *J* = 17.2, 1.5 Hz, 1H), 5.28 (dt, *J* = 10.4, 1.2 Hz, 1H), 5.21 (s, 2H), 4.68 (dt, *J* = 5.9, 1.3 Hz, 2H), 4.20 (ddd, *J* = 7.6, 5.3, 4.0 Hz, 1H), 3.22 (q, *J* = 6.6 Hz, 2H), 2.75 (d, *J* = 5.6 Hz, 1H), 1.90-1.59 (m, 2H), 1.56-1.38 (m, 3H). <sup>13</sup>C NMR (100 MHz, CDCl<sub>3</sub>) δ 175.0, 133.7, 131.5, 129.9, 129.7, 129.5, 127.0, 119.4, 77.4, 70.4, 66.4, 64.1, 41.0, 34.0, 29.7, 22.1.



**Allyl (2S)-2-((((tert-butoxycarbonyl)leucyl)oxy)-6-((((2-chlorobenzyl)oxy)carbonyl)amino)hexanoate (S11)** was synthesized according *General procedure B* using **S10** (279 mg, 0.78 mmol) and Boc-Leu-OH (361 mg, 1.56 mmol). **S11** was obtained as a colorless oil (379 mg, 85%). <sup>1</sup>H NMR (400 MHz, CDCl<sub>3</sub>) δ 7.44-7.35 (m, 2H), 5.89 (ddtd, *J* = 17.2, 10.4, 5.8, 2.7 Hz, 1H), 5.32 (dq, *J* = 17.2, 1.5 Hz, 1H), 5.27-5.19 (m, 2H), 5.04 (s, 1H), 4.95-4.80 (m, 1H), 4.62 (dp, *J* = 5.6, 1.4 Hz, 2H), 4.34 (s, 1H), 3.21 (s, 2H), 1.96-1.63 (m, 4H), 1.56-1.37 (m, 12H), 1.26 (d, *J* = 2.6 Hz, 2H), 0.97-0.85 (m, 6H). <sup>13</sup>C NMR (100 MHz, CDCl<sub>3</sub>) δ 187.4, 156.4, 140.2,

131.5, 129.6, 127.0, 126.1, 119.2, 81.6, 80.2, 66.1, 64.0, 41.5, 32.0, 29.2, 28.5, 24.9, 22.8, 14.3.



**(2S)-2-(((tert-butoxycarbonyl)leucyl)oxy)-6-(((2-chlorobenzyl)oxy) carbonyl)amino)hexanoic acid (S12)** was synthesized according *General procedure C* using **S11** (365 mg, 0.64 mmol) and **S12** was obtained as a yellow solid (320 mg, 94%)  $^1\text{H}$  NMR (400 MHz,  $\text{CDCl}_3$ )  $\delta$  7.69-7.63 (m, 1H), 7.58-7.53 (m, 1H), 7.48 – 7.44 (m, 1H), 7.39 (ddd,  $J = 16.9, 5.2, 2.6$  Hz, 2H), 5.18-4.84 (m, 3H), 4.31 (s, 1H), 3.20 (d,  $J = 6.3$  Hz, 2H), 1.97-1.61 (m, 4H), 1.60-1.45 (m, 5H), 1.43 (s, 9H), 0.98-0.90 (m, 6H).  $^{13}\text{C}$  NMR (100 MHz,  $\text{CDCl}_3$ )  $\delta$  173.0, 172.6, 156.2, 136.6, 132.2, 131.4, 129.5, 128.5, 126.8, 80.2, 72.2, 63.9, 41.0, 40.8, 30.5, 29.3, 28.3, 24.7, 22.9, 21.7.



## Detailed Methods

**General peptide synthesis.** Unless otherwise stated amino acids and reagents were purchased from either Iris Biotech or Sigma Aldrich. Peptides were synthesized by SPPS using a 9-fluorenylmethyloxycarbonyl (Fmoc) strategy at 0.1-0.25 mmol scale. Preloaded 4-benzyloxybenzyl alcohol (Wang) resins (Iris Biotech) were used. Standard coupling reactions were achieved with 1:4:4:8 [resin: N-protected amino acid (AA): 2-(1-benzotriazole-1-yl)-1,1,3,3-tetramethyluronium hexafluorophosphate (HBTU), *N,N*-diisopropylethylamine (DIPEA)] or 1:4:4:8 [resin: AA: 1-(bis(dimethylamino)methylene)-1*H*-1,2,3-triazolo(4,5-*b*)pyridinium 3-oxid hexafluorophosphate (HATU): collidine]. Coupling reactions were agitated at room temperature (RT) and monitored using a Kaiser test (Sigma Aldrich). Deprotections were carried out with 20% piperidine (2 × 2 min). After coupling or deprotection steps the resin was extensively washed with dimethylformamide (DMF).

**Automated peptide synthesis.** Automated peptide synthesis following Fmoc-SPPS was carried out on a Liberty Blue microwave peptide synthesizer (CEM, Matthews, NC, USA) with 30 mL Teflon reaction vessel using preloaded Wang-resin (100–200 mesh). Reagents were prepared as solutions in DMF: Fmoc-protected amino acids (0.2 M), *N,N'*-diisopropylcarbodiimide (DIC) in DMF (0.5 M) and ethyl 2-cyano-2-(hydroxyimino)acetate (Oxyma) in DMF (1.0 M). Microwave assisted sequence elongation was achieved using the following protocol: deprotection (150W, 15 s, 75°C, followed by 30W, 60 s, 90°C), coupling (190W, 180 s, 75°C, followed by 36W, 120 s, 90°C). Amino acids were double coupled using amino acid/DIC/Oxyma (ratio 1:1:1) in 5-fold excess over the resin loading to achieve peptide elongation.

**Fluorescence labeling.** N-terminal labeling of peptides with carboxytetramethylrhodamine (TAMRA) was carried out by SPPS. TAMRA was coupled on resin at RT for 16 h using a mixture of 1.5:1.5:3 [5(6)-TAMRA (Anaspec Inc.): benzotriazol-1-yloxy)tripyrrolidinophosphonium hexafluorophosphate (PyBOP): DIPEA] dissolved in *N*-methyl-2-pyrrolidone (NMP).<sup>6</sup> The reaction vessels were covered to avoid

photo bleaching of the fluorophore and the resin was extensively washed with DMF and DCM after coupling.

**Depsipeptide synthesis.** Depsipeptides were either synthesized by Fmoc-SPPS strategy as described above or by tert-butyloxycarbonyl (Boc)-SPPS. For Boc-SPPS, a 2-(tritylmercapto)acetyl-L-leucinyloxyphenylacetamidomethyl (PAM) resin was used to generate all thioester depsipeptides and preloaded PAM resins (Peptides International) were used for Boc-SPPS depsipeptides. Couplings were achieved as described above and deprotection of the N-terminal Boc protection group was achieved by treating the resin with neat trifluoroacetic acid (TFA) (1 × 1 min). The resin was washed extensively with DMF and DCM after each coupling or deprotection step.

$\alpha$ -Hydroxy acids were either purchased from Sigma Aldrich or synthesized as described (Supplementary Methods). Coupling of  $\alpha$ -hydroxy acids was carried out by dissolving the  $\alpha$ -hydroxy acid (5.5 eq) in a 1:1 mixture of (DCM:DMF, 4 mL) on ice followed by addition of *N,N'*-diisopropylcarbodiimide (DIC) (5 eq) and 1-hydroxy-benzotriazole (HOBt) (6 eq). After 15 min the mixture was added to the resin along with *N*-ethyl-morpholine (NEM) (2 eq), followed by agitating for 20 min at RT. The resin was washed extensively with DMF and DCM. Ester bond formation was achieved by pre-mixing the subsequent Boc-protected AA (5.5 eq) in a mixture of DCM and DMF (1:1, 1 mL) on ice and DIC (5 eq) for 15 min, after which the mixture was added to the resin followed by addition of *N,N'*-dimethylpyridin-4-amine (DMAP) (0.1 eq) and NEM (2 eq) and agitated for 1 h at RT. The resin was washed extensively with DCM and DMF and the coupling step was repeated twice. Boc-AA-O-AA-OH building blocks were synthesized as described (Supplementary Methods). Coupling of building blocks were performed using conventional SPPS coupling conditions as described above.

**Cyclic peptide synthesis.** Resin bound linear peptides with orthogonally protected allyl (All) amines and allyloxycarbonyl (Alloc) carboxyl residues were flow-washed with DCM and drained. All- and Alloc-protecting groups were removed using tetrakis(triphenylphosphane)palladium(0) (Pd(PPh<sub>3</sub>)<sub>4</sub>) (0.2 eq) and phenylsilane (PhSiH<sub>3</sub>) (20 eq) in dry DCM (1 mL) for 15 min with agitation. After flow-washing with

DCM, the procedure was repeated. Complete removal of protecting groups was confirmed by using a Kaiser test (Sigma Aldrich) and test cleavage in neat TFA followed by LC-MS analysis. Next, the resin was swelled in DMF (10 min), flow-washed with DMF and side chain to side chain cyclization (lactam formation) was achieved using PyBOP (2.0 eq) and DIPEA (2.0 eq) in DMF (1 mL) agitating until completion of the cyclization reactions followed by LC-MS after test cleavage in neat TFA.

**Peptide cleavage and purification.** Fmoc-peptides were cleaved from the resin using a mixture of 95:2.5:2.5 (TFA:H<sub>2</sub>O:triisopropylsilane (TIPS)) for 2 h at RT. Boc-peptides were cleaved using a hydrogen fluoride (HF)-reaction apparatus (Peptides International) in a mixture of 9:1 (HF:p-cresol) for 1-2 h at 0°C. After cleavage the peptides were precipitated in ice-cold diethyl ether. The precipitate was centrifuged (3.500 rpm, 3-30 min, 4°C), washed with cold diethyl ether and the centrifugation step was repeated. The resulting peptide precipitate was dissolved in 50:50:0.1 (acetonitrile (MeCN):H<sub>2</sub>O:TFA), filtered and lyophilized.

All peptides were purified using a preparative reverse phase high performance liquid chromatography (RP-HPLC) system (Waters) with a reverse phase C18 column (Zorbax, 300 SB-C18, 21.2 × 250 mm). A linear gradient using a binary buffer system of H<sub>2</sub>O:MeCN:TFA (A: 95:5:0.1; B: 5:95:0.1) at 20 mL/min was used. Collected fractions were characterized by electron spray ionization (ESI) liquid chromatography mass spectrometry (LC-MS) coupled to an Agilent 6410 triple quadrupole with a reverse phase C18 column (Zorbax Eclipse XBD-C18, 4.6 × 50 mm) using a binary buffer system consisting of H<sub>2</sub>O:MeCN:formic acid (A: 95:5:0.1; B: 5:95:0.1) at 0.75 mL/min. The purity of the collected fractions was measured at 214 nm on an analytical reverse phase ultra-performance liquid chromatography (RP-UPLC) (Waters) system with a reverse phase C18 column (Acquity UPLC BEH C18, 1.7 μm 2.1 × 50 mm) using a binary buffer system consisting of H<sub>2</sub>O:MeCN:TFA (A: 95:5:0.1; B: 5:95:0.1) at 0.45 mL/min. The final peptide products were lyophilized. In case of oxidized methionine, the purified peptide was dissolved in TFA and reduced as described previously<sup>7</sup>. After reduction TFA was evaporated under nitrogen and the peptide was diluted in H<sub>2</sub>O:MeCN:TFA (50:50:0.1) and purified using preparative RP-HPLC as described above.

**Vector design.** The human Mint2 (hMint2) DNA was obtained from Life Technologies and incorporated into a pRSET vector containing a poly histidine tag. hMint2 PARM (364-570) was amplified by PCR using primers encoding XhoI (5'-CGGCGGCTCGAGCATCGAGGGTCGCAAAGAACTGCAGCTGG-3') and BamHI (5'-CGGCGGGGATCCTCATCAGGTGGTCACCGGCG-3') restriction sites. The PCR product was purified, digested with XhoI and BamHI and ligated into the pRSET vector, using Rapid DNA ligation kit (Roche). The C-terminal fragment PARM (479-570) ( $\Delta_C$ PARM) used in expressed protein ligation (EPL) was incorporated into a pET vector containing a poly histidine tag using primers encoding a FXa protease site and BamHI (5'-CGGCGGGGATCCATCGAAGGCCGCTGCAGCCAGGATGCCATTG-3') and XhoI (5'-GGTACGCTCGAGTTATTACTGCAGTTCTTTGGCG-3') restriction sites. Using the same approach as described above, the PCR product was purified, digested and inserted into the pET vector. The N-terminal PARM (364-452) thioester fragment ( $\Delta_N$ PARM) used in EPL was generated using the primers (5'-GTTTAACTTTAAGAAGGAGATATACATATGGAAGATCTGATTGATGGTATTATCTTTGC-3'), (5'-CGGCAGTGCAACTAATGCATCACCGGTAATACAATGATCCATCATGGTTTCTTGGGTATC-3') . The primer contains an overhang sequence corresponding to the intein Mxe-GyrA<sub>mini</sub>,<sup>8</sup> which was used to generate a mega primer using PARM (364-570) as template. The generated mega primer was used to introduce  $\Delta_N$ PARM into a pTXB1 vector containing the same overhang sequence coding for Mxe-GyrA<sub>mini</sub>. The pTXB1 vector contains an N-terminal polyhistidine tag to retain the cleaved intein after thiolysis using reverse His purification. Side chain mutation was introduced by a standard site-directed mutagenesis protocol (Stratagene). All sequences were verified by DNA sequencing (GATC Biotech).

**Expression and purification.** The plasmids were transformed into *E. coli* BL21(DE3)pLysS (Invitrogen) and grown on Luria broth (LB)-agar plates containing ampicillin (100  $\mu$ g mL<sup>-1</sup>) at 37°C overnight. A few colonies were transferred to 100 mL LB-medium including ampicillin (100  $\mu$ g mL<sup>-1</sup>) and incubated for 16 h at 30°C. Subsequently, the cells were transferred to either 0.5 L or 1 L LB medium containing ampicillin (100  $\mu$ g mL<sup>-1</sup>) to give an OD<sub>600nm</sub> of 0.1 and incubated at 37°C. When an OD<sub>600nm</sub> between 0.4-0.6 was reached, the expression cultures were induced with 0.1 mM isopropyl  $\beta$ -D-thiogalactoside (IPTG) at 37°C for

4 h or 18°C overnight. After induction, cells were harvested by centrifugation (10.000 x g, 10 min, 4°C) and kept at -20°C until use.

The His-tagged PARM mutants were purified by suspending the pellets into lysis buffer [50 mM NaP<sub>i</sub>, 10 mM MgCl<sub>2</sub>, 25 µg/mL DNase, cOmplete protease inhibitor tablets (1 tab/50 mL) (Roche), pH 7.4] and disrupted by passing the lysate through a cell-disruptor system (Constant System Ltd) at 26 kPsi. Subsequently, cell debris was removed by centrifugation (30.000 x g, 30 min, 4°C) and the supernatant was loaded using a peristaltic pump onto 5 mL HisTrap columns (GE Healthcare Life Science). Before and after loading the sample, the columns were equilibrated or washed with wash buffer (20 mM imidazole, 150 mM NaCl, 25 mM HEPES, pH 7.4), respectively. Next, the protein was eluted with elution buffer (250 mM imidazole, 150 or 500 mM NaCl, 25 mM HEPES, pH 7.4). The eluted protein was loaded onto a HiLoad 16/600 Superdex 75 pg column (GE Healthcare) and buffer exchanged into storage buffer (150 or 500 mM NaCl, 25 mM HEPES, pH 7.4). 500 mM NaCl was used to achieve a higher protein concentration. All proteins were characterized by ESI-LC-MS (Agilent, Poroshell, 300SB-C18, 2.1 × 75 mm) and the purity was determined by analytical RP-HPLC (Agilent 1100) or RP-UPLC (Waters Acquity) (Table S4).

For purification of the C-terminal PARM (479-570) fragment, the HisTrap eluate was dialyzed into Factor-Xa cleavage buffer (25 mM HEPES, 50 mM NaCl, 1 mM CaCl<sub>2</sub>, pH 7.4) at 4°C, using SnakeTubes (Sigma Aldrich) with a molecular cutoff on 10.000 Da. Factor Xa, 1 UN/3mg protein (Haematologic Technologies) was added to the sample to generate the desired Cys-terminal fragment after 72 h at 4°C. After cleavage, the sample was loaded onto 5 mL HisTrap columns and eluted with wash buffer to retain the His-tagged part of the protein. Finally, the eluted protein was purified using a reversed phase C4 column (YMC-Pack-C4, 250 × 20 mm) and lyophilized.

The N-terminal PARM (364-452) thioester was purified by adding solid GdnHCl to the lysis buffer after cell disruption to generate a final concentration of 6 M GdnHCl. The protein sample was centrifuged (50.000 x g, 1.5 h, 4°C) and the supernatant was filtered and loaded onto 2 × 5 mL HisTrap columns. The protein was purified as described above except for addition of 6 M GdnHCl in all buffers. After elution, the protein sample was dialyzed into intein cleavage buffer (25 mM HEPES, 500 mM NaCl, 2 M urea, pH 7.0) using SnakeTubes (Sigma Aldrich, 10.000 Da MWCO). Then 2-mercaptoethanesulfonic acid sodium salt

(MesNa) was added to reach a final concentration of 200 mM and thiolysis was allowed for 48 h at 4°C at pH 7.0. Subsequently, the pH was elevated to 7.4 and the sample was loaded onto 2 × 5 mL His-trap columns and eluted with wash buffer to retain the Mxe-GyrA<sub>mini</sub> intein and uncleaved protein. The eluted PARM (364-452) thioester protein was then precipitated by dialyzing into water. Finally, the precipitate was centrifuged (3.500 x g, 10 min, 4°C), the supernatant removed and the protein precipitate washed with water. This was repeated three times and the resulting protein precipitate was lyophilized and characterized by LC-MS (Agilent) and UPLC (Waters).

**Expressed protein ligation.** Ligations of all semisynthetic proteins were initiated by dissolving 1 eq of lyophilized  $\Delta_c$ PARM (0.5  $\mu$ mol) and 1.5 eq of lyophilized synthesized thioester peptides ( $\Delta_{pep}$ PARM) (0.75  $\mu$ mol) in 1 mL ligation buffer [6 M GdnHCl, 200 mM NaPi, 100 mM mercaptophenyl acetic acid (MPAA), 17 mM TCEP, pH 6.5] + 5% MeOH to increase solubility of  $\Delta_{pep}$ PARM. After 8 h at RT, 200 mM methoxy amine was added to the Eppendorf tube and conversion of Thz to Cys was performed overnight at RT. Subsequently, the ligation mixture was buffer exchanged using Amicon ultra centrifugal filters (10 MWCO, Sigma Aldrich) into ligation buffer. The second ligation was conducted by dissolving 1 eq of lyophilized  $\Delta_N$ PARM (0.5  $\mu$ mol) in ligation buffer and adding this to the ligation mixture. After overnight incubation at RT, the ligated protein was purified using a reverse phase C4 column (Jupitor, Phenomenex, 250 × 10 mm) and lyophilized. After lyophilization, desulfurization was conducted by dissolving the semisynthetic protein in desulfurization buffer (6 M GdnHCl, 200 mM NaPi, 100 mM TCEP, 40 mM glutathione, 20 mM VA-044 radical initiator, pH 6.0). Reaction was allowed at RT for 48 h. After quantitative conversion of Cys to Ala as monitored by LC-MS, the semisynthetic protein was refolded into storage buffer (500 mM NaPi, 25 mM HEPES, pH 7.4) using a HiLoad 16/600 Superdex 75 pg column (GE Healthcare). The purity was determined by RP-UPLC (Waters) at 214 nm, the mass was confirmed by LC-MS (Agilent) and the concentration was determined by NanoDrop 1000 (Thermo Fisher Scientific) (Table S3).

**Circular dichroism.** CD experiments were performed on an Olis DSM 100 (Olis Inc.) CD spectrometer in a 1 mm quartz cuvette using a protein concentration of 15  $\mu$ M in 150 or 500 mM NaCl, 25 mM HEPES at pH 7.4. Data were obtained in millidegrees ellipticity ( $m^\circ$ ) and converted to mean residue ellipticity ( $\theta_{MRE}$ ) using the following equation (1):

$$\theta_{MRE} = \frac{m^\circ}{L [\text{Protein}] n} \quad (1),$$

where [Protein] is the concentration of protein in molar, n = number of backbone amides in the protein and L = path length of cuvette in mm.

**ThermoFluor.** ThermoFluor experiments were done in a 96-wells plate format on a Stratagene Mx3005p qPCR cycler (Agilent). 15  $\mu$ M protein in 20  $\mu$ L 500 mM NaCl, 25 mM HEPES, pH 7.4 was mixed with 1x SYPRO Orange as final concentration and heated by increasing the temperature by 1°C starting from 25°C and ending at 95°C. After each heating step the sample was excited at 492 nm and emission at 610 nm was detected.

**Fluorescence polarization.** The binding affinities were determined in a flat bottom black 384-well plate (Corning Life Science) using a Safire<sup>2</sup> plate reader (Tecan). All experiments were conducted in 150 or 500 mM NaCl, 25 mM HEPES, 1% bovine serum albumin (BSA), pH 7.4 at 25°C and the fluorescence was measured at excitation/emission wavelength at 530/580 nm. The instrumental Z-factor was adjusted to maximum fluorescence and the G-factor was calibrated to give an initial millipolarization at 20. FP assays were either performed as saturation (for semisynthetic proteins and side chain mutated proteins) or competition experiments (for mutated APP peptides) using TAMRA-APP<sub>17-mer</sub> [(TAMRA)-NNG-QNGYENPTYKFFEQMQN] as probe at a concentration of 50 nM.

For saturation experiments, the protein was measured at 11 different concentrations by making 1:1 dilutions. All experiments were done in triplicate and the data was fitted to a one-site binding model. In the competition experiments, a preformed complex of PARM/TAMRA-APP<sub>17-mer</sub> was outcompeted with unlabeled peptides at 12 different concentrations ranging from 0.24-500  $\mu$ M. The experiments were

performed in triplicate and the data were fitted to a sigmoidal dose response curve using GraphPad Prism 7. The  $K_i$  value was calculated according to Nikolovska-Coleska et al.<sup>9</sup> If either the  $K_d$  or  $K_i$  value was high (>100  $\mu$ M) the  $B_{max}$  or  $B_{min}$  values were constrained to the corresponding value of the WT measurement.

**Rat Mint2<sup>Y460A/F521A</sup> cloning.** Using the QuikChange II Site Directed Mutagenesis kit (Agilent Technologies) pEGFP-Mint2<sup>Y460A/F521A</sup> was created stepwise from rat pEGFP-Mint2 using the following primers:

Y460A forward: 5'-GCCTTGCGCACCATCTCCGCCATTGCAGACATTGGGAAC-3'

reverse: 5-'GTTCCCAATGTCTGCAATGGCGGAGATGGTGCGCAAGGC-3'

F521A forward: 5'-GTCAATTGGGCAGGCCGCCAGTGTGGCCTACCAG-3'

reverse: 5'-CTGGTAGGCCACACTGGCGGCCTGCCCAATTGAC-3'

For expression in neurons, pEGFP-Mint2<sup>Y460A/F521A</sup> mutant was subcloned into the lentiviral pFUW vector and sequenced verified. Also see SI Appendix, Figure S11 for sequence alignment.

**HEK293T co-immunoprecipitation.** 48 h following transfection using FuGENE6 (Roche), human embryonic kidney (HEK) 293T cells were lysed in immunoprecipitation buffer containing: 10 mM Tris HCl pH 8.0, 150 mM NaCl, 1 mM EDTA pH 8.0, and 1% Triton X-100, supplemented with protease inhibitors (Roche). Protein extracts were incubated for 2 h with rotation at 4°C with the precipitating antibody (rabbit anti-Mint2 1:200; Sigma M3319) followed by overnight incubation with 20  $\mu$ L of protein A Ultralink resin (Thermo Scientific). The resin was washed several times with immunoprecipitation buffer and precipitated proteins were eluted by boiling for 5 min in reducing SDS sample buffer and resolved by SDS-PAGE. The following antibodies were used for immunoblotting: APP (mouse; Sigma 22C11, 1:500), GFP (rabbit; Cederlane Labs 132002, 1:1000), tubulin (mouse; Cell Signaling 3873, 1:1000).

**Primary neuron infection with Mint2<sup>Y460A/F521A</sup> and A $\beta$  ELISA.** Primary neuronal cultures were prepared from newborn (P0) mice of either sex carrying a double transgene for mutant APP or presenilin-1 and infected with lentivirus for Mint2<sup>Y460A/F521A</sup> two days after plating as previously described.<sup>10</sup> Briefly, neurons were dissociated with trypsin, triturated, and plated onto wells coated with Matrigel (Corning). Recombinant



lentiviruses were produced by transfecting HEK293T cells using FuGENE6 (Roche) with plasmids encoding viral enzymes and envelope proteins essential for packing of viral particles (RSV/REV, MDLg/RRE, and VSVG) with the addition of a shuttle vector encoding the gene of interest (pFUW).

At DIV15, neuronal lysate was collected in reducing SDS sample buffer and resolved by SDS-PAGE. The following antibodies were used for immunoblotting: APP (mouse; Sigma 22C11, 1:500), Mint2 (rabbit; Sigma M3319, 1:1000), tubulin (mouse; Cell Signaling 3873, 1:1000). Media was also collected at 15 DIV) and handled according to the protocol of the Human A $\beta$ <sub>42</sub> Ultrasensitive ELISA Kit (Invitrogen, Cat. No. KHB3544) following colorimetric readout at 450 nm. Results were compared to neurons containing endogenous Mints 1-3 (control), set to 100% normalized A $\beta$ <sub>42</sub> concentration (pg/mL). The data is presented as mean + SEM of 7 biological replicates from 2 independent experiments.

***In vitro* plasma stability.** Human plasma was preheated at 37°C for 15 min before spiked with a final concentration of 0.25 mM of **1**, KSL-221036 or APP<sub>WT</sub>. Samples were collected after 0, 1, 2, 4, 6 and 24 h or after 0, 2, 5, 10, 30 and 60 min, depending on stability. The compounds were extracted by pre-treatment with 6 M urea (10 min) followed by addition of 20% trichloroacetic acid (TCA) and incubation (10 min). The samples were centrifuged at 13,400 rpm for 10 min and the supernatant was analyzed by RP-UPLC (Waters) at 214 nm. The area under the curve (AUC) was determined and normalized to the first time point. The half-life (T<sub>1/2</sub>) was determined by fitting the data to a one-phase decay equation in Prism 7.0. The data is represented as the mean of three individual experiments.

***In vitro* hepatic clearance.** Mouse hepatic microsomes (Life Technologies) were incubated with 1 mM NADPH, 3 mM MgCl<sub>2</sub> and 5 mM KSL-221036 and APP<sub>WT</sub> at 37°C. Samples were collected after 0, 5, 10, 15, 30, 45 and 60 min. The compounds were extracted by pre-treatment with 6 M urea (10 min) followed by addition of 100  $\mu$ L acetonitrile (ACN). The samples were centrifuged at 13,400 rpm for 10 min and the supernatant was analyzed by RP-UPLC (Waters) at 214 nm. The AUC was determined and normalized to the first time point. The data was fitted to a one-phase decay equation to determine the T<sub>1/2</sub>. The intrinsic

clearance ( $CL_{(int)}$ ) was determined using the elimination rate constant  $k$ . Propranolol was used a positive control.

**Isothermal titration calorimetry (ITC).** The experiments were performed using an ITC200 (Malvern). In brief, experiments were conducted at 25°C and 1.000 rpm. stirring and designed so that  $C$  values were generally within 10–200 ( $C$  value =  $K_A \times [\text{protein}] \times N$ , with  $K_A$ , equilibrium association constant;  $[\text{protein}]$ , protein concentration in the cell;  $N$ , stoichiometry). Ligand-to-buffer titrations were performed to subtract the heat produced by injection, mixing and dilution. The binding enthalpy was directly measured, while the dissociation constant ( $K_D$ ) and stoichiometry ( $N$ ) were obtained by data analysis using the Origin software (OriginLab) (SI Appendix Fig. S13).

**MTS cytotoxicity assay.** To analyze the neuronal cytotoxicity of **14** (KSL-221036, no CPP), **15** (TAT<sup>47-57</sup>-**14**), **16** (mixTAT-**14**), **17** (polyArg-**14**), **19** (MiniAp4-**14**) and **20** (TAT-APP<sub>WT</sub>), DIV15 primary neurons from newborn (P0) mice carrying transgene for mutant APP and presenilin-1 were treated with a concentration curve of peptide, as indicated. PBS and DMSO were used as solvent for the peptides, and final concentration of DMSO in the 20  $\mu$ M treatment wells was 0.5% (v/v). 20% (v/v) DMSO, known to induce cytotoxicity, was used as positive control. After 24 h incubation at 37°C, cell viability was measured by CellTiter96® AQueous One Solution Cell Proliferation Assay kit (Promega). Results were compared to untreated neurons, set to 100% viability (SI Appendix Fig. S15).

**Covalent immobilization of peptides.** Peptides KSL-221036 and APP<sub>WT</sub>, comprising a C-terminal Cys and PEG<sub>2</sub> linker, were loaded covalently to Dynabeads M-270 Epoxy beads (Thermo Fischer Scientific) according to the protocol of the manufacturer. The peptides were dissolved in coupling buffer (1 mg of peptide is dissolved in 60  $\mu$ L DMSO, 300  $\mu$ L 100 mM PBS buffer containing 2 M (NH<sub>4</sub>)SO<sub>4</sub> and 6.2  $\mu$ L of 0.5 M TCEP in MQ water, pH = 7,4) and agitated overnight at 37°C with Dynabeads M-270 Epoxy beads, which had been washed and equilibrated with coupling buffer before. After removing excess peptides, the

Dynabeads M-270 Epoxy beads were washed three times and equilibrated with 100 mM PBS buffer, pH = 7.4 and stored at 4°C.

**Protein isolation from neuronal cell lysate.** The peptide-loaded beads were incubated, washed and eluted in Eppendorf tubes using a magnetic rack for separation. Primary neuronal cultures were prepared from transgenic (*Mint1*<sup>-/-</sup>; *Mint2*<sup>fl/fl</sup>; *Mint3*<sup>-/-</sup>) newborn (P0) mice and infected with lentivirus two days after plating as described above. Control neurons containing *Mint2* were infected with a lentiviral inactive *cre* recombinase, while *Mint2* knockout neurons were infected with active *cre* recombinase. At 15 DIV neurons were lysed in immunoprecipitation buffer containing: 10 mM Tris HCl pH 8.0, 150 mM NaCl, 1 mM EDTA pH 8.0, and 1% Triton X-100, supplemented with protease inhibitors (Roche). In brief, neuronal cell lysate was incubated with the loaded beads for 2 h at 37°C. After washing the beads 5 times with PBS buffer (4 × 1 mL PBS, pH 7.4, 1 × 1 mL PBS with 0.5% Triton X-100, pH 7.4), the beads were eluted with 15 µL 2x sample reducing buffer. The eluate was collected in clean tubes, boiled (100°C, 5 min) resolved by SDS-PAGE. The following antibodies were used for immunoblotting: *Mint2* (rabbit; Sigma M3319, 1:1,000) and GAPDH (mouse; Millipore Sigma MAB374, 1:5,000). Three individual experiments were performed (SI Appendix Fig. S14).

**Aβ<sub>42</sub> ELISA and LDH cytotoxicity assay following peptide treatment.** Primary neuronal cultures were prepared from newborn (P0) mice of either sex carrying two alleles of a double transgene for mutant APP or presenilin-1 as described above. **14** (KSL-221036, no CPP), **15** (TAT<sup>47-57</sup>-**14**), **16** (mixTAT-**14**), **17** (polyArg-**14**), **19** (MiniAp4-**14**) and **20** (TAT-APP<sub>WT</sub>) as well as DAPT were prepared as stock solutions in DMSO and diluted using either neuronal cell medium or PBS buffer according the desired final concentration in the assay. Neuronal cell medium was equilibrated to 500 µL before addition of peptide solutions. At 14 DIV, neurons were incubated with peptides, DAPT ( $\gamma$ -secretase inhibitor) and vehicle control (0.25% DMSO) for 24 h at 37°C. The cell medium was collected, diluted and handled according to the protocol of the Human Aβ<sub>42</sub> Ultrasensitive ELISA Kit (Invitrogen, Cat. No. KHB3544) following colorimetric readout at 450 nm. Results were compared to the application of the solvent (vehicle control,

0.25% (v/v) DMSO), set to 100% normalized A $\beta$ <sub>42</sub> concentration (pg/mL). The data is presented as mean + SEM (SI Appendix Fig. S16). The same media used was evaluated for toxicity using the CyQUANT™ LDH Cytotoxicity Assay (Thermo Fisher Scientific). Results were compared to the application of the solvent (vehicle control, 0.25% (v/v) DMSO), set to 100% normalized LDH release. The data is presented as mean + SEM of three biological replicates (SI Appendix Fig. S16).

**Immunocytochemistry following peptide treatment.** Primary hippocampal cultures were prepared from newborn (P0) mice of either sex carrying transgene for mutant APP or presenilin-1 and plated on glass coverslips. On 6 DIV, neurons were treated with **14** (10  $\mu$ M, no CPP) and **15** (5  $\mu$ M, TAT<sup>47-57</sup>-**14**) for 24 h. At the end of the 24 h, neurons were fixed with 4% paraformaldehyde at RT for 8 min, washed 3 times with PBS, and then permeabilized and blocked in 10% goat serum and 0.1% saponin in PBS for 1 h at RT. Incubation with mouse anti-HIV1 TAT [N3] primary antibody (Abcam 63957 at 1:500) in blocking buffer (10% goat serum in PBS) occurred overnight at 4°C. Neurons were then washed 3 times with PBS and incubated with goat anti mouse IgG secondary antibody conjugated to Alexa Fluor-488 (Invitrogen 1:500) in blocking buffer (10% goat serum in PBS) for 1 h at RT. Following PBS washes, the coverslips were mounted using ProLong Gold Antifade Mountant with DAPI (Invitrogen) and imaged with a Carl Zeiss LSM 700 confocal microscope at 63X magnification (SI Appendix Figure S17).

**Molecular dynamics simulations.** The Mint2/APP system was minimized and enclosed in a simulation box of desired volume and solvated using predefined or custom solvent models under periodic boundary conditions. All atoms in the system were assigned random velocities using the Maxwell-Boltzmann distribution. This was followed by an equilibration step where the temperature of the system was slowly increased to the desired temperature, rescaling the velocities if needed. Then, the trajectory was recorded by predicting atom coordinates for each frame of the simulation keeping constant pressure and temperature. The output trajectory contained all structural data for each recording, referred to as frames.

MD simulation experiments were first designed on a system consisting of the concerned peptide ligand in complex with the Mint2-PTB domain. Once the cyclized peptides attained a relaxed conformation in the

binding site, a representative helical conformation of the peptide ligand only was extracted from the trajectory of the complex. Then a similar MD simulation experiment was performed with only the solvated peptide to assess the stability of the peptide conformation in solution. Each MD simulation was 200 ns long and run in duplicates. A simulation interaction diagram (SID) was employed to classify each residue of the peptide ligand for each frame as part of a helix or not. A Python script was used to parse the data file to quantify the percent of frames containing a helix. Presence of a helix was defined as a frame containing at least 4 continuous helical residues. The number of helical frames was used to define helical propensity and the average of the helical propensity across the simulations was defined as follows (2):

$$\text{helical propensity} = \frac{\text{number of helical frames} * 100}{\text{total number of frames}} \% \quad (2)$$

Simulations were performed at 300 K using force field OPLS3 and solvent system Tip3p.

**Data analysis.** All data analysis was performed in GraphPad Prism 7.0 (GraphPad Inc.), Excel 2010 (Microsoft) and Origin 9.0 (OriginLab). Significance was evaluated using Student's *t*-test in case of two groups; the one-way ANOVA test was used in case of three or more groups, combined with either Dunnett's or Sidak's multiple comparison test.

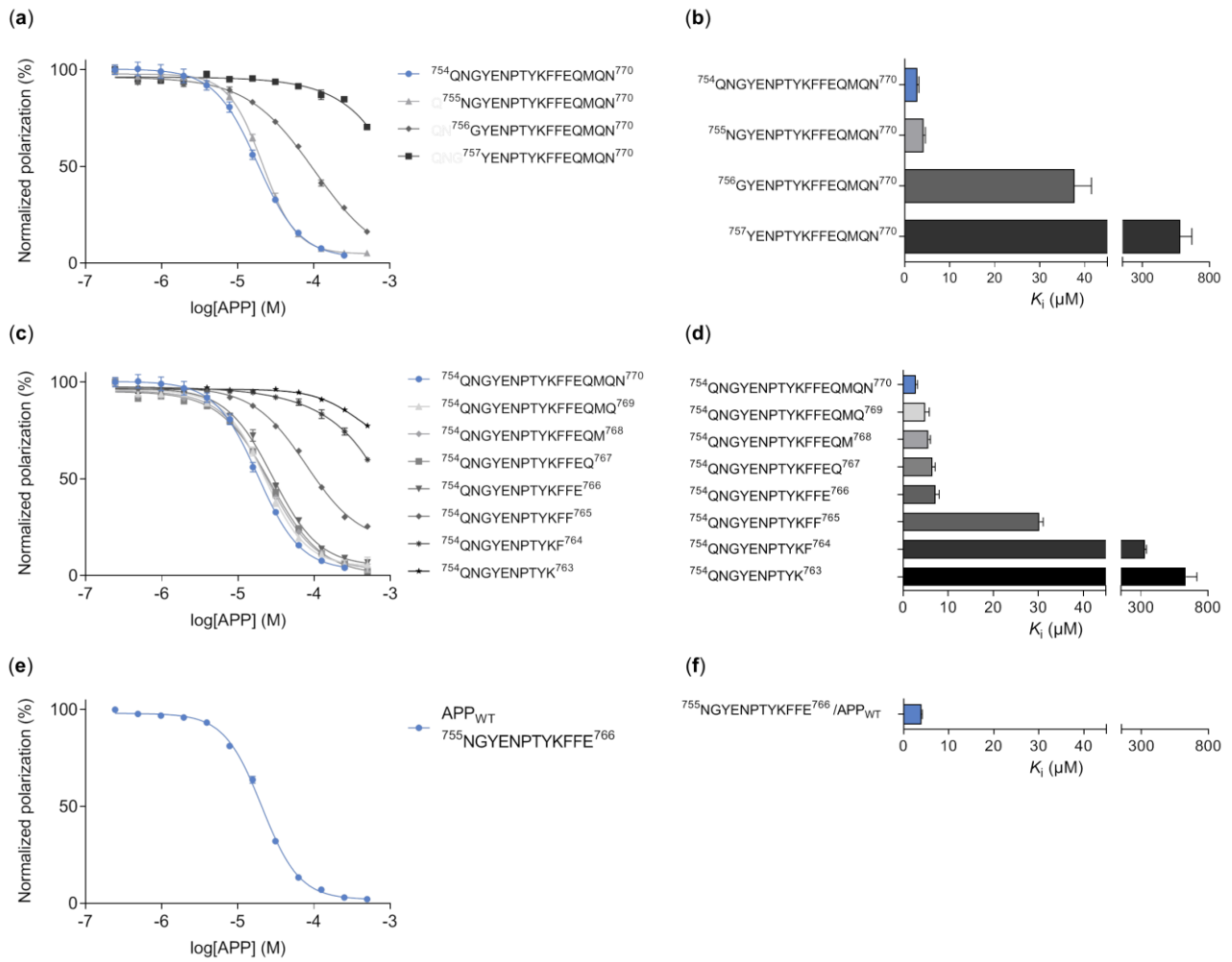


**Figure S1. The affinity of the human 17-mer APP peptide.** QNGYENPTYKFFEQM<sup>Q</sup><sub>770</sub>; residues 754–770, blue) as well as N- and C-terminal truncated APP peptides towards Mint2-PARM measured by FP. (a) FP inhibition curves of the binding of APP N-terminal truncations. (b)  $K_i$  values of APP N-terminal truncations (mean + SEM, n = 3). (c) FP inhibition curves for the binding of APP C-terminal truncations. (d)  $K_i$  values of APP C-terminal truncations (mean + SEM, n = 3). (e) FP inhibition curve for the binding of the minimal binding sequence of APP (termed APP<sub>WT</sub>). (f)  $K_i$  value of the minimal binding sequence of APP (termed APP<sub>WT</sub>) (mean + SEM, n = 3).

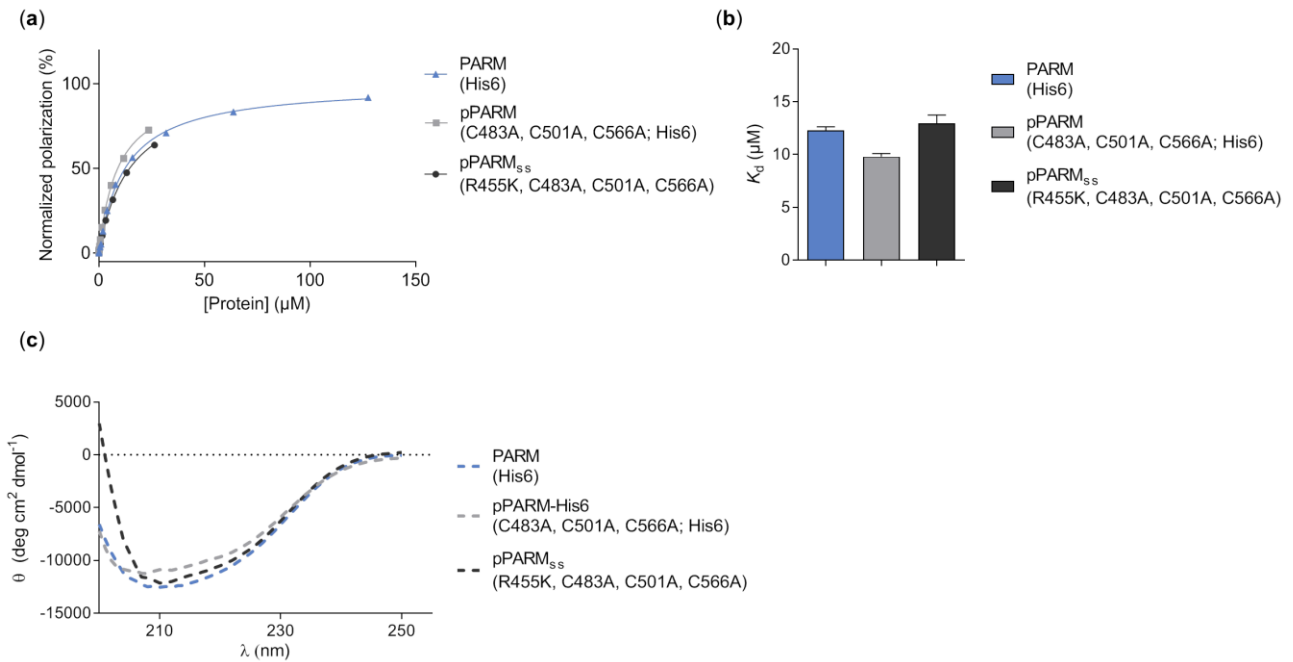


**Figure S2. Binding data and comparison of secondary structure of Mint2-PARM variants.** (a) FP saturation curves of the binding of APP<sub>C-term</sub> to Mint2-PARM variants. (b)  $K_d$  values of APP<sub>C-term</sub> binding to Mint2-PARM variants (mean + SEM,  $n = 3$ ). (c) CD spectra recorded from 250–200 nm in mean residue ellipticity (MRE) ( $\text{deg cm}^2 \text{dmol}^{-1}$ ), data presented as average of three individual measurements ( $n = 3$ ).

#### Overview of Mint2-PARM variants:

- **PARM** (residue: 364–570; His6-tag)
- **pPARM** (residues: 364–570; mutations: R455K, C483A, C501A, C566A; His6-tag)  
Intention: prepared to have similar mutations as the pPARM<sub>ss</sub> construct.
- **pPARM<sub>ss</sub>** (residues: 364–570; mutations: R455K, C483A, C501A, C566A; no His6-tag and a Met as first amino acid)  
Intention: prepared to compare as reference to the A-to-E variants of pPARM<sub>ss</sub>)

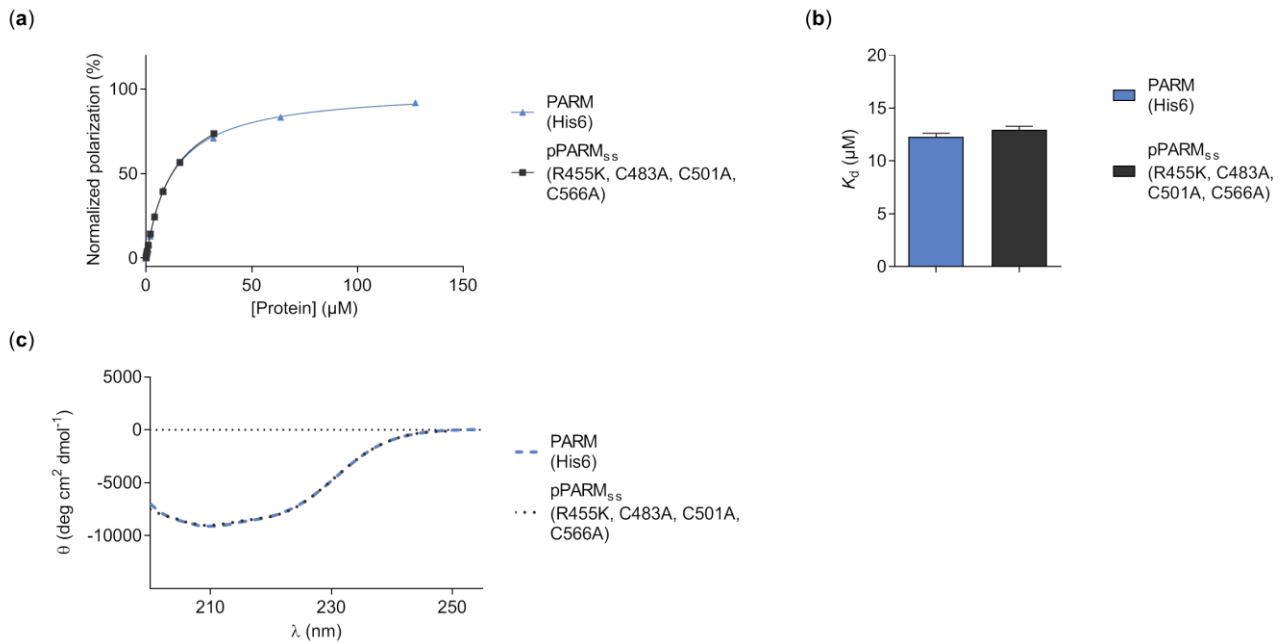


**Figure S3. Binding data and comparison of secondary structure of expressed Mint2-PARM and Mint2-pPARM<sub>ss</sub>.** (a) FP saturation curves of APP<sub>C-term</sub> binding to expressed Mint2-PARM and semisynthetic Mint2-pPARM<sub>ss</sub>. (b)  $K_d$  values of APP<sub>C-term</sub> binding to expressed Mint2-PARM and Mint2-pPARM<sub>ss</sub> (mean + SEM, n = 3). (c) CD spectra recorded from 250–200 nm in MRE (deg cm<sup>2</sup> dmol<sup>-1</sup>), data presented as average of three individual measurements (n = 3). FP and CD confirm that expressed Mint2-PARM and semisynthetic Mint2-pPARM<sub>ss</sub> have similar binding affinities to APP<sub>C-term</sub> and similar secondary structure.



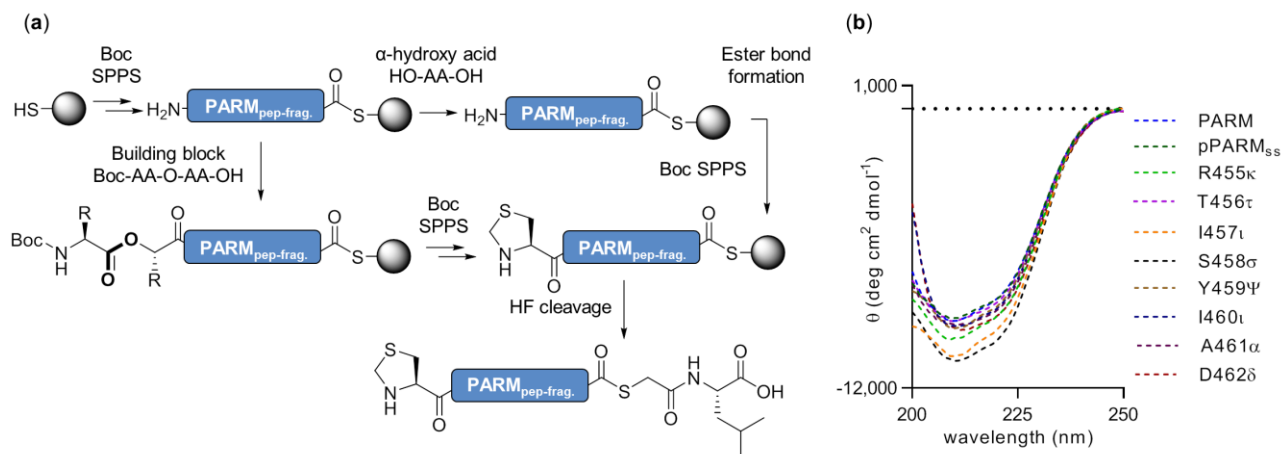


**Figure S4. Synthesis of depsipeptide fragment  $\Delta_{\text{pep}}\text{PARM}$  (A453-S478) and secondary structure of Mint2-pPARM<sub>SS</sub> A-to-E variant.** (a) Synthesis of the central peptide fragment  $\Delta_{\text{pep}}\text{PARM}$  (A453-S478) is achieved through Boc-SPPS on preloaded PAM resin containing a free thiol. The ester bond is either introduced by coupling of the corresponding  $\alpha$ -hydroxy acid followed by ester bond formation on resin, or by coupling of a preformed depsipeptide building block. Global deprotection and cleavage off the resin is achieved using HF. (b) CD spectra of Mint2 pPARM<sub>SS</sub> A-to-E variants recorded from 250–205 nm shown as mean-residue-ellipticity (MRE) ( $\text{deg cm}^2 \text{ dmol}^{-1}$ ) ( $n = 3$ ).

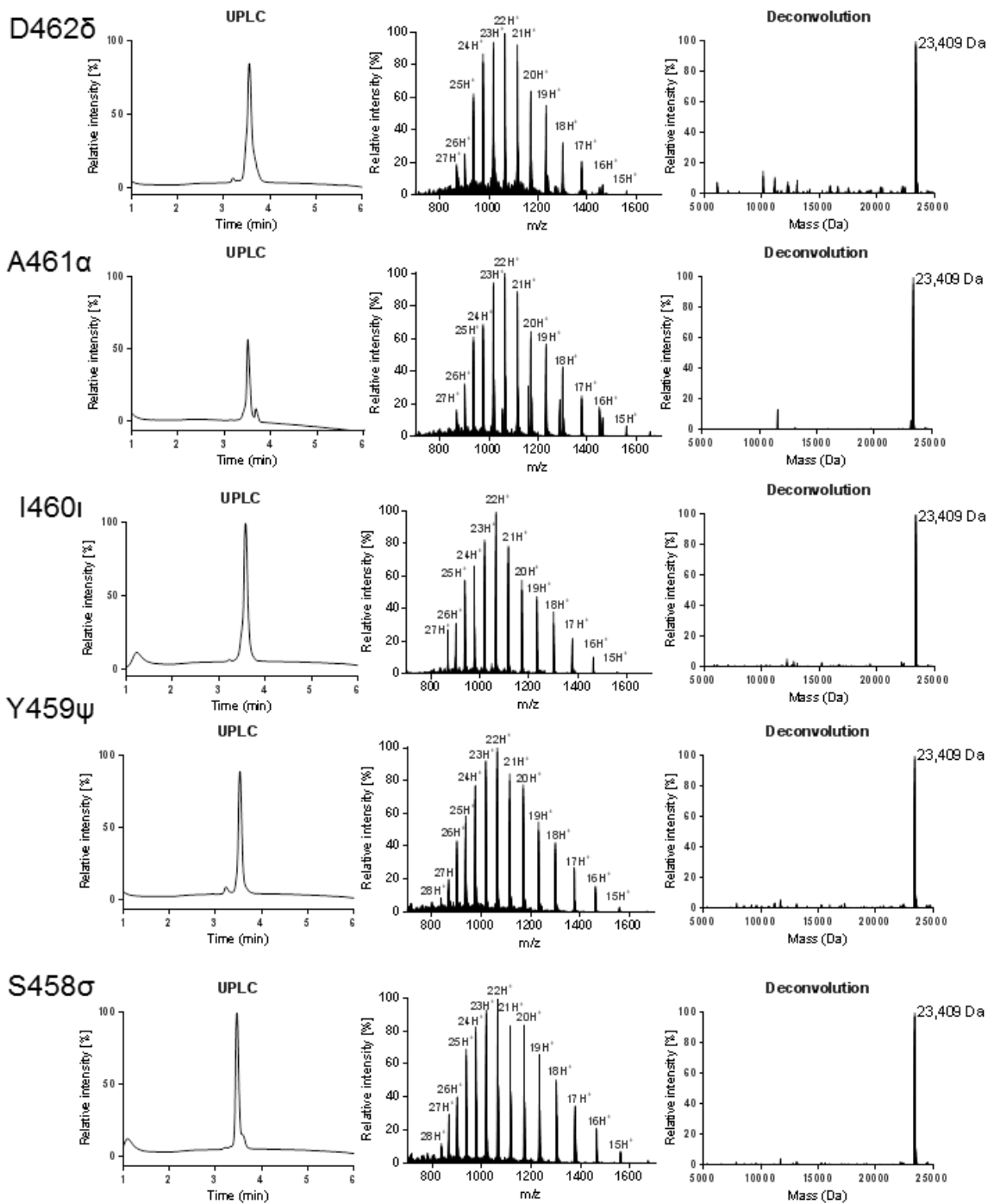


**Figure S5. Characterization of Mint2-pPARMss A to-E variants by UPLC and LC-MS.** (see legend below)

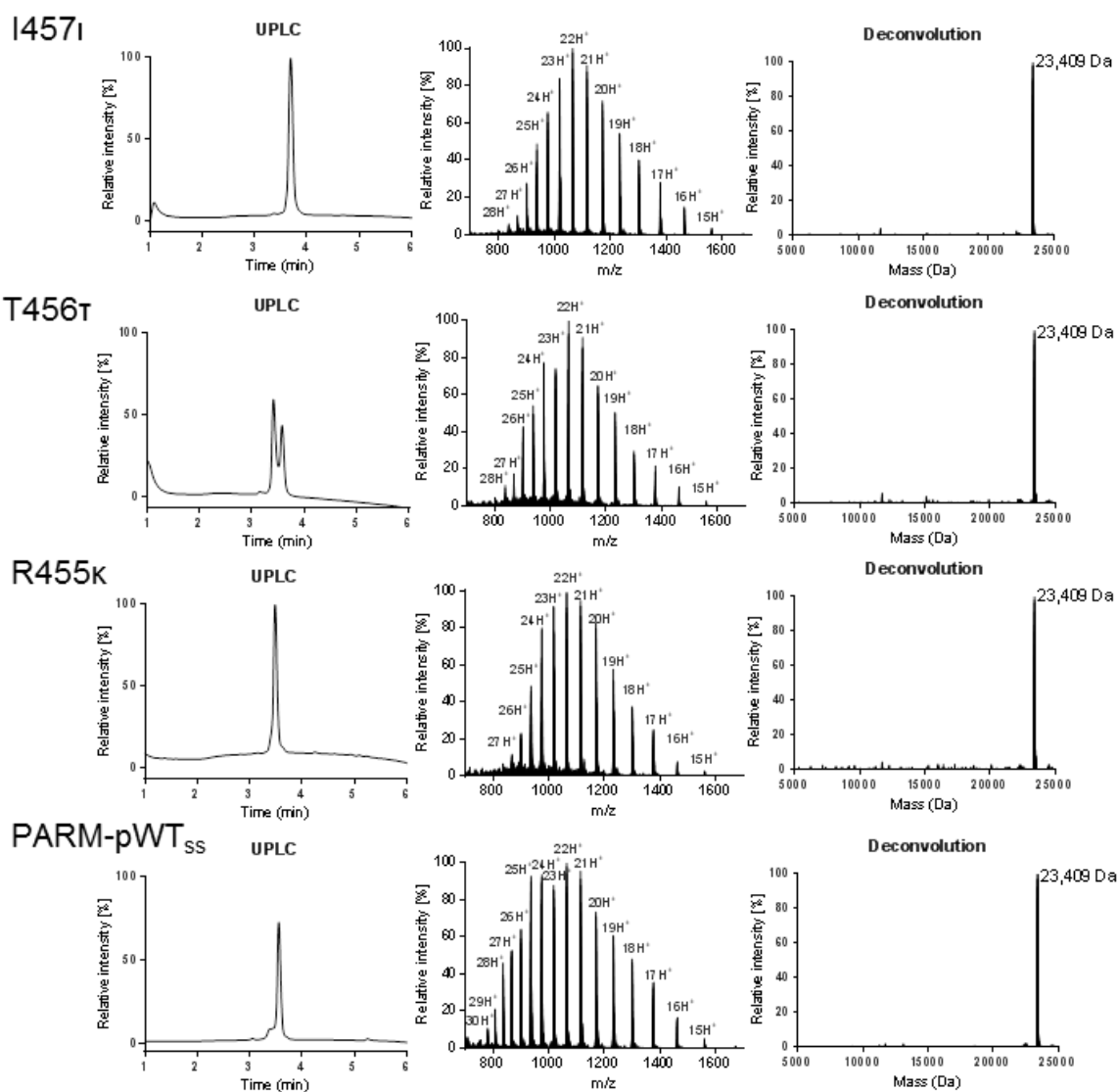


**Figure S5. Characterization of Mint2-pPARM<sub>ss</sub> A-to-E variants by UPLC and LC-MS.** The Mint2-pPARM<sub>ss</sub> A-to-E substitution is indicated above each dataset consisting of three chromatograms; left: UPLC UV trace (214 nm); middle: LC-MS MS spectrum (ESI); right: deconvoluted mass [expected mass: 23,410 Da (Mint2-pPARM<sub>ss</sub>) and 23,411 Da (Mint2-pPARM<sub>ss</sub> A-to-E variants)]. Note that UPLC chromatogram of T456τ shows in a double peak, which could be due to racemization of the side chain, as only one peak and mass was seen by SEC purification and LC-MS analysis, respectively.

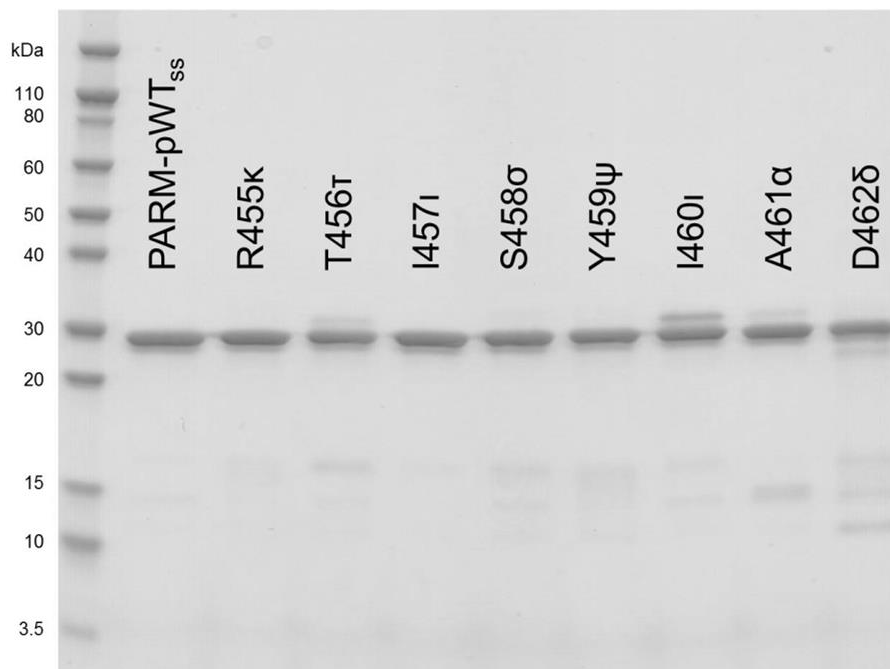


**Figure S6. SDS-PAGE of Mint2-pPARG<sub>ss</sub> A-to-E variants.** 16% RunBlue SDS-PAGE gel, (expected mass: 23,410 Da).

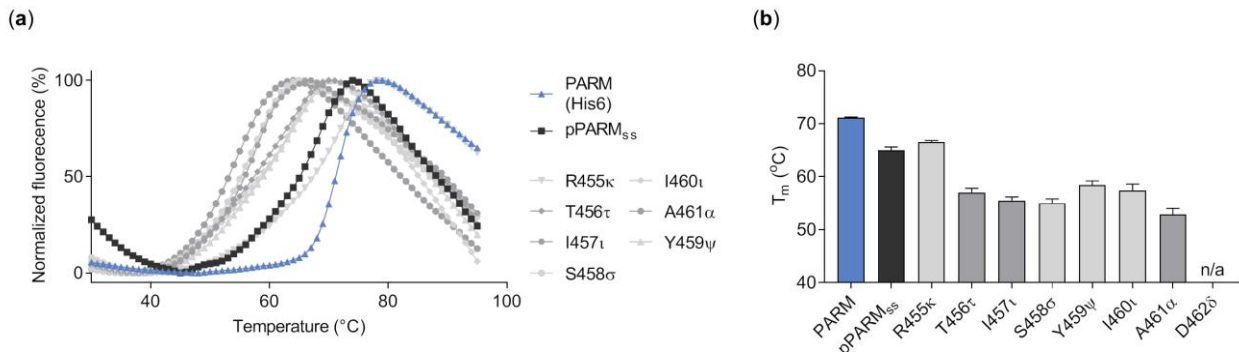


**Figure S7. Effect of A-to-E substitutions on the melting temperature ( $T_m$ ) of pPARM<sub>SS</sub> variants.** SYPRO Orange was used to obtain protein melting curves of the pPARM<sub>SS</sub> A-to-E variants from 25°C to 95°C. (a) Normalized ThermoFluor plots. No data was obtained from D462δ as the ester bond hydrolyzed at increased temperatures. (b) Bar diagram of melting  $T_m$  in C, data presented as mean + SEM ( $n = 3$ ); n/a = not available.

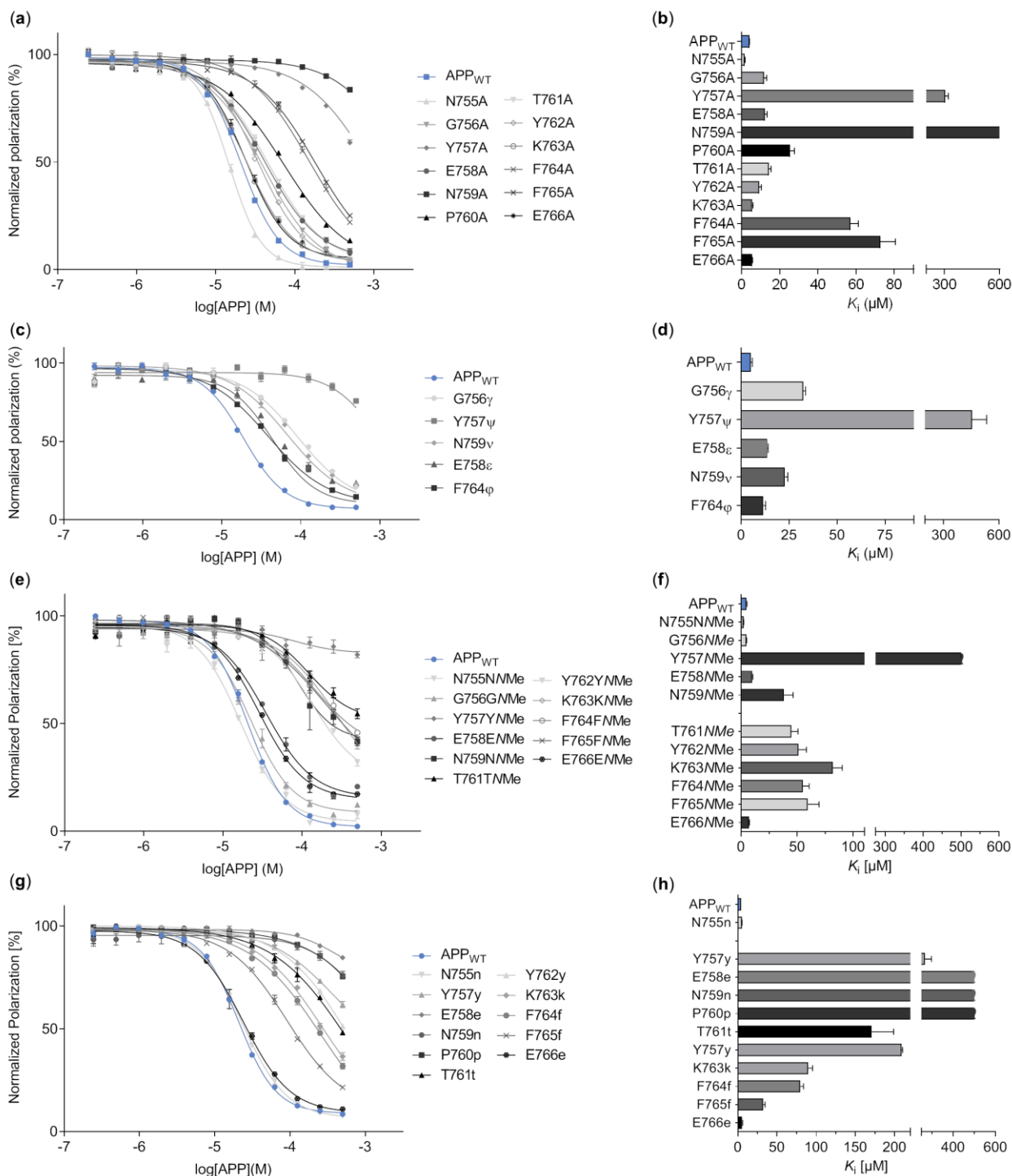


**Figure S8. Binding affinities of Ala, A-to-E, D-AA and NMe-AA variants of APP<sub>WT</sub>.** Affinities of the 12-mer APP<sub>WT</sub> peptide NGYENPTYKFFE (APP<sub>770</sub>; residues 755–766, blue) and its variants were measured using FP and Mint2-PARM. (a) Inhibition curves of the binding of APP<sub>WT</sub> Ala substitutions. (b)  $K_i$  values of APP<sub>WT</sub> Ala substitutions. (c) Inhibition curves of the binding of APP<sub>WT</sub> A-to-E substitutions. (d)  $K_i$  values of APP<sub>WT</sub> A-to-E substitutions. (e) Inhibition curves of the binding of APP<sub>WT</sub> NMe-AA substitutions. (f)  $K_i$  values of APP<sub>WT</sub> NMe-AA substitutions. (g) Inhibition curves of the binding of APP<sub>WT</sub> D-AA substitutions. (h)  $K_i$  values of APP<sub>WT</sub> D-AA substitutions. Data expressed as mean + SEM (n = 3).

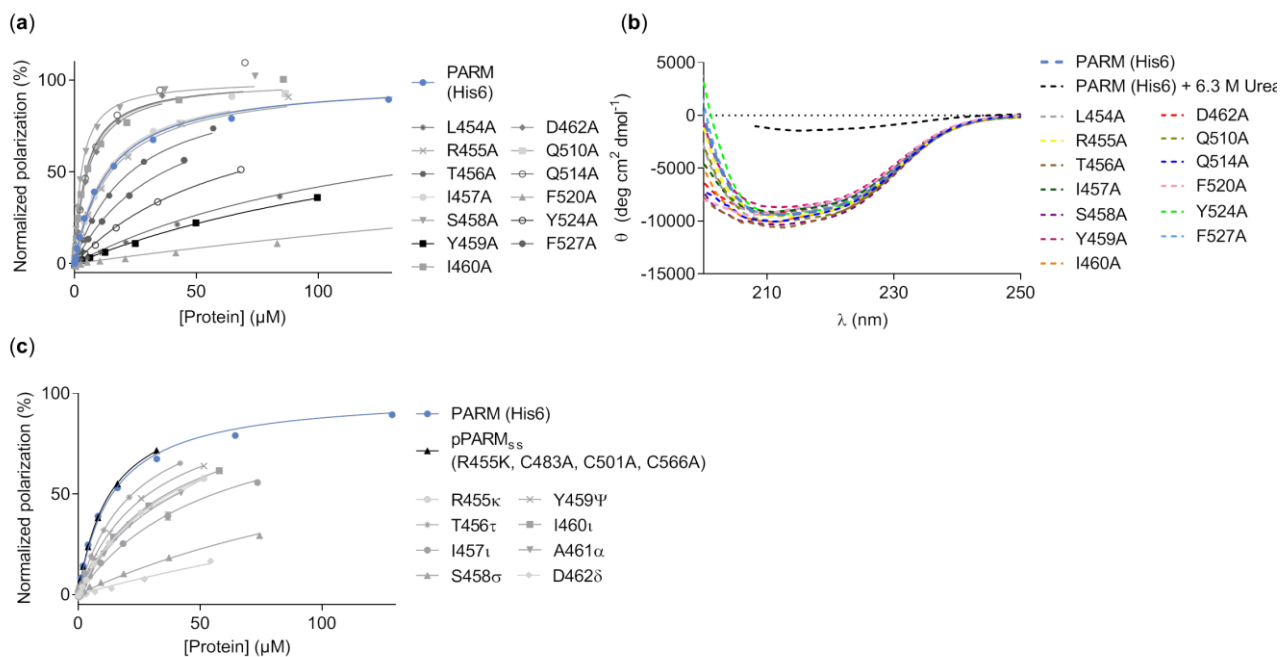


**Figure S9. Binding and secondary structure characterization of Mint2-PARM Ala and Mint2-pPARM<sub>SS</sub> A-to-E variants.** Affinities of Mint2-PARM Ala and Mint2-pPARM<sub>SS</sub> A-to-E variants towards APP<sub>WT</sub> peptide measured by FP. (a) Saturation curves of the binding of the APP<sub>WT</sub> peptide to Mint2-PARM Ala variants. (b) CD spectra of Mint2-PARM Ala variants recorded from 250-200 nm in MRE ( $\text{deg cm}^2 \text{dmol}^{-1}$ ); data presented as average of three individual measurements. (c) Saturation curves of the binding of the APP<sub>WT</sub> peptide to Mint2-pPARM<sub>SS</sub> A-to-E variants; data is presented as mean  $\pm$  SEM ( $n = 3$ ).

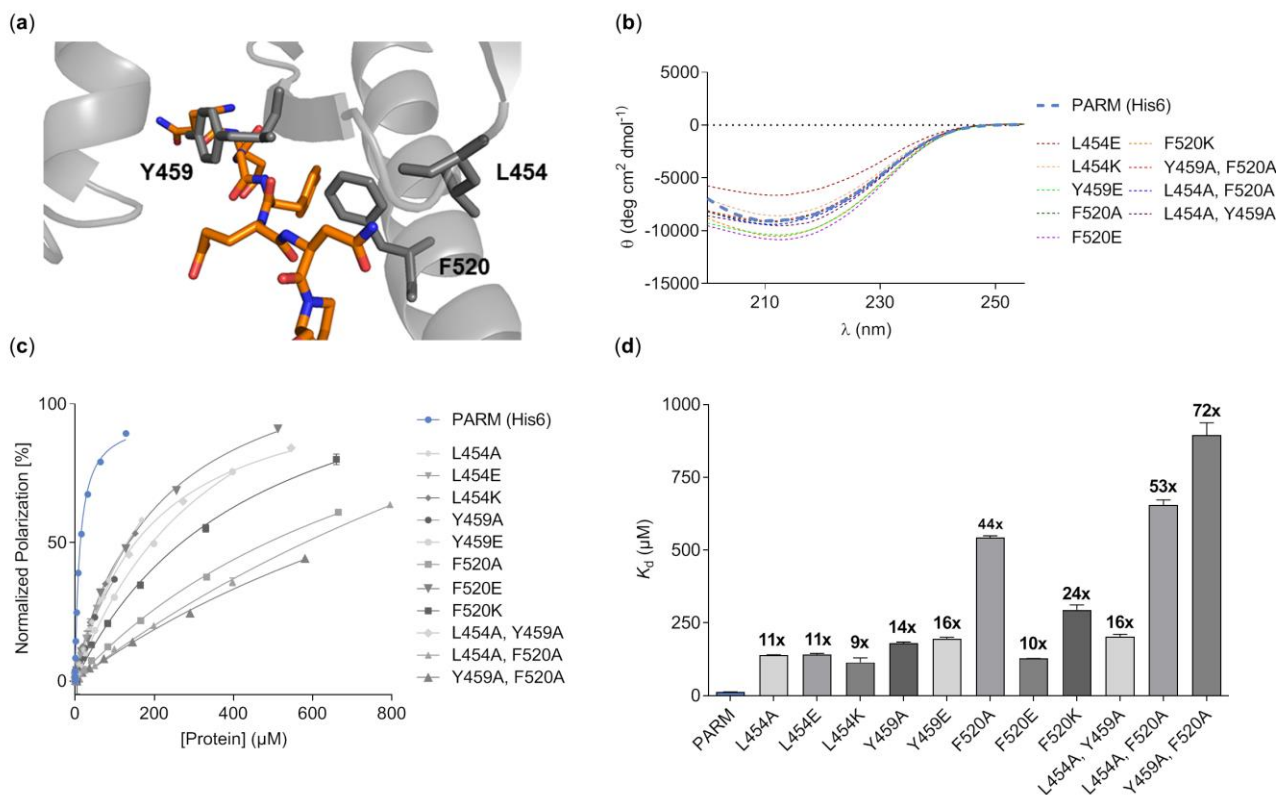


**Figure S10. Mutational scan of L454, Y459 and F520 in Mint2-PARM.** 12 variants were expressed, and 11 characterized by FP and CD as the Y459K variant did not express as soluble protein. (a) X-ray crystal structure of rat Mint2-PARM (grey) co-crystallized with APP (orange). Probed positions in Mint2-PARM are highlighting as sticks (PDB ID: 3SV1).<sup>11</sup> (b) CD spectra recorded from 250-200 nm in MRE (deg cm<sup>2</sup> dmol<sup>-1</sup>); data presented as average of three individual measurements. (c) Normalized FP saturation curves of the interaction between the APP<sub>WT</sub> peptide and Mint2-PARM variants (mean ± SEM, n = 3). (d) K<sub>d</sub> values and fold change (K<sub>d</sub>(variant)/K<sub>d</sub>(wild type)) of the Mint2-PARM variants relative to Mint2-PARM (mean + SEM, n = 3).



```

APBA1_HUMAN MNHLEGSAEVEVTDEAAGGEVNESVEADLEHPEVEEEQQQPPQQQHYVGRHQGRGLE 58
APBA2_RAT MAHRKRQSTASSMLDHRARPGPIPHDQEPENE-----DTELP-LESYV---PTGLELG 49
APBA2_HUMAN MAHRKLESVSGSMLDHRVRPGVPVPHSQEPESE-----DMELP-LEGYV---PEGLELA 49
APBA3_HUMAN -----

APBA1_HUMAN DLRAQLGQEEEEERGECLARSASTE--SGFHNHTDTAEGDVIAAARDGYDAERAQDPEDES 116
APBA2_RAT TLRPDSP--TPEEQECHNHSPDGDSSSDYVNNT-----SEEEDYDE-GLPEEEEEGV 97
APBA2_HUMAN ALRPESP--APEEQECHNHSPDGDSSSDYVNNT-----SEEEDYDE-GLPEEEEEGI 97
APBA3_HUMAN -----

APBA1_HUMAN AYAVQYRPEAEYETEQAEEAEHAETHRRALPNHLHFHSLHEEEAMNAAYSQYVYTHRLFH 176
APBA2_RAT TYYIRYCPEDDSYLEGMDCNGEYLAHGAHPVDTD----ECQEA-VEDWTDSVGPHTSH 152
APBA2_HUMAN TYYIRYCPEDDSYLEGMDCNGEYLAHSAHPVDTD----ECQEA-VEEWTDSAGPHPHGH 152
APBA3_HUMAN -----

APBA1_HUMAN RGEDEPYSEPYADYGGLOEHVYEEIGDAPELDARDGLRLYEQERDEAAAYRQEALGARLH 236
APBA2_RAT GAEN---SQEYPDS-----HLP-----IPE-DDPTVLEVVDQEEED--GHYCPSK-ESYQD 195
APBA2_HUMAN EAEG---SQDYPDG-----QLP-----IPE-DEPSVLEAHDQEEED--GHYCASK-EGYQD 195
APBA3_HUMAN -----M 1

APBA1_HUMAN HYDERSDGEDSDSPEK-----EAEFAPY----PRMDSYEQEEDIDQIVA 275
APBA2_RAT YYPPEYNGNT-----GGASPYRMRRGDGDLEEQEEDIDQIVA 232
APBA2_HUMAN YYPEEANGNT-----GASPYRLRRGDGDLEDQEEDIDQIVA 231
APBA3_HUMAN DFPTISRSPSGPPAMDLEGPRDILVPSEDLTPDSQWDPMFG--GPGSLSRMELDE----- 54
      :   : . :                               *           .       * *

APBA1_HUMAN EVKQSMSSQSLDKAAEDMPEAEQDLERPPTPAGGRPDSPLQAPAGQORAVGPAGGGEAG 335
APBA2_RAT EIKMSLSMTSITSASEASPEHMPPELDPGDSTEACSPS-----DTGRGP 275
APBA2_HUMAN EIKMSLSMTSITSASEASPEHGPEPGPEDSVEACPPI-----KASCSP 274
APBA3_HUMAN -----SSLQELVQQFEALPGDL---VGPSPG-GAPCPLHI-----ATGHGL 91
      *  . : . * * : * . .

APBA1_HUMAN QSYS-KEKRDAISLAIKDIKEAIEEVKTRTIRSPYTPDEPKPIWVMRQDISPTRDCDDQ 394
APBA2_RAT SRQEARPKSLNLPPEVKHSGDPQRGLKTKT-----RTPEERPKWPQEQVCNGLEQPRKQ 329
APBA2_HUMAN SRHEARPKSLNLLPEAKHPGDPQRGFKPKT-----RTPEERLKWPHQEQVCNGLEQPRKQ 328
APBA3_HUMAN ASQEIADAHGLLSA--EAGRDDLGLLH-CEECPPSQTGPEEPLEPAPRLLQPPEDPDED 148
      . : : : . : . : . :

APBA1_HUMAN R----PMDGDSPS-PGSSS-PLGAESSSTSLHPSDPVEASTNKESTRKSLASFPTYVEVPG 448
APBA2_RAT Q----R-----S-DL-----NGP-TDNNNIPETKKVASFPSFVAVPG 360
APBA2_HUMAN Q----R-----S-DL-----NGP-VDNNNIPETKKVASFPSFVAVPG 359
APBA3_HUMAN SDSPEWVEGASAEQEGSRSSSSPEPWLETVPLVTPEEPPAGAQPETLASYPAPQEVPG 208
      *                               *           . . : : * * *

APBA1_HUMAN PCDPEDLIDGIIFAANYLGSTQLLSDKTPSKNVRMMQAQEAVSRKMAQKLAQRKK-AP 507
APBA2_RAT PCEPEDLIDGIIFAANYLGSTQLLSERNPSKNIRMMQAQEAVSRVKRMQKAAKIKKKANS 420
APBA2_HUMAN PCEPEDLIDGIIFAANYLGSTQLLSERNPSKNIRMMQAQEAVSRVKRMQKAAKIKKKANS 419
APBA3_HUMAN PCDHEDLLDGVIFGARYLGSTQLVSEPNPTSTRMAQAREAMDRVK-----AP 256
      ** : ** : ** : ** : * . ***** : * : . * .. ** ** : ** : * : *

```

**Figure S11. Sequence alignment of Mint proteins.** (see explanation below)

```

APBA1_HUMAN EGESQPMTEVDLFIISTQRIKVLNADTQETMMDHPLRTISYIADIGNIVVLMARRRMPRSN 567
APBA2_RAT EGDAQTLTEVDLFIISTQRIKVLNADTQETMMDHALRTISYIADIGNIVVLMARRRMPRSA 480
APBA2_HUMAN EGDAQTLTEVDLFIISTQRIKVLNADTQETMMDHALRTISYIADIGNIVVLMARRRMPRSA 479
APBA3_HUMAN DGETQPMTEVDLFLVSTKRIKVLTAADSQEAMMDHALHTISYTADIGCVLVLMARRRLARRP 316
      :*:* * :*****:**:*****.**:**:* ** * :***** *
      :*:* * :*****:**:*****.**:**:* ** * :***** *

APBA1_HUMAN SQENVEASHPSQDGKRQYKMICHVFESEDAQLIAQSIGQAFSVAYQEFLRANGINPEDLS 627
APBA2_RAT SQDCIETTPGAQEGKKQYKMICHVFESEDAQLIAQSIGQAFSVAYQEFLRANGINPEDLS 540
APBA2_HUMAN SQDCIETTPGAQEGKKQYKMICHVFESEDAQLIAQSIGQAFSVAYQEFLRANGINPEDLS 539
APBA3_HUMAN -----APQDHGRRLYKMLCHVFYAEDAQLIAQAIGQAFAAAYSQFLRESGIDPSQVG 368
      :*:* * :*****:**:*****.**:**:* ** * :***** *

APBA1_HUMAN QKEYSDLNLTQDMYNDDLIHFSKSENCKDVFIEKQKGEILGVVIVESGWSILPTVILAN 687
APBA2_RAT QKEYSDIINTQEMYNDDLIHFSNSENCKELQLEKHKGEILGVVVESGWSILPTVILAN 600
APBA2_HUMAN QKEYSDIINTQEMYNDDLIHFSNSENCKELQLEKHKGEILGVVVESGWSILPTVILAN 599
APBA3_HUMAN VHPS---PGACHLHNGDLDHFSNSDNCREVHLEKRRGEGLGVALVESGWSLLPTAVIAN 425
      : : : :*.** ***:**:*: :**:* ***.:**:*****:**:***:***

APBA1_HUMAN MMHGGAEPKSGKLNIGDQIMSINGTSLVGLPLSTCQSIKGLKNQSRVKNIVRCPPVTT 747
APBA2_RAT MMNGGPAARSGKLSIGDQIMSINGTSLVGLPLATCQGIKGLKNQTQVKNIVSCPPVTT 660
APBA2_HUMAN MMNGGPAARSGKLSIGDQIMSINGTSLVGLPLATCQGIKGLKNQTQVKNIVSCPPVTT 659
APBA3_HUMAN LLHGGAEPKSGALSIGDRLTAINGTSLVGLPLAACQAAVRETKSQTSVTLSIVHCPPVTT 485
      :*:*** :** *.***:*: :*****:**:***. : : *.*: *.*** *****

APBA1_HUMAN VLIRRPDLRYQLGFSVQNGIICSLMRGGIAERGGVVRVGHRIIEINGQSVVATPHEKIVHI 807
APBA2_RAT VLIKRPDLKYQLGFSVQNGIICSLMRGGIAERGGVVRVGHRIIEINGQSVVATAHEKIVQA 720
APBA2_HUMAN VLIKRPDLKYQLGFSVQNGIICSLMRGGIAERGGVVRVGHRIIEINGQSVVATAHEKIVQA 719
APBA3_HUMAN AIIHRPHAREQLGFCVEDGIICSLLRGGIAERGGIRVGHRIIEINGQSVVATPHARIEL 545
      :*:*** : *****.*:*****:*****:*****:*****:*****:***** * :*:.

APBA1_HUMAN LSNAVGEIHMKTMPAAMYRLLTAQEQPVYI 837
APBA2_RAT LSNSVGEIHMKTMPAAMFRLLTGQETPLYI 750
APBA2_HUMAN LSNSVGEIHMKTMPAAMFRLLTGQETPLYI 749
APBA3_HUMAN LTEAYGEVHIKTMPAATYRLLTGQEQPVYL 575
      *:*: **:*:***** :*****.** *:*:

```

**Figure S11.** Sequence alignment of Mint proteins. Residues Y459 and F520 substituted to alanine yielding APP non-binding human Mint2<sup>Y459A/F520A</sup> or rat Mint2<sup>Y460A/F521A</sup> are highlighted in blue. Sequence identity of rat Mint2 (APBA2\_RAT) by running *blastp* (BLASTP 2.7.1+) against Human Mint2 (APBA2\_HUMAN) via UniProt is 92,3% (<https://www.uniprot.org/>, accessed 04.01.2019).

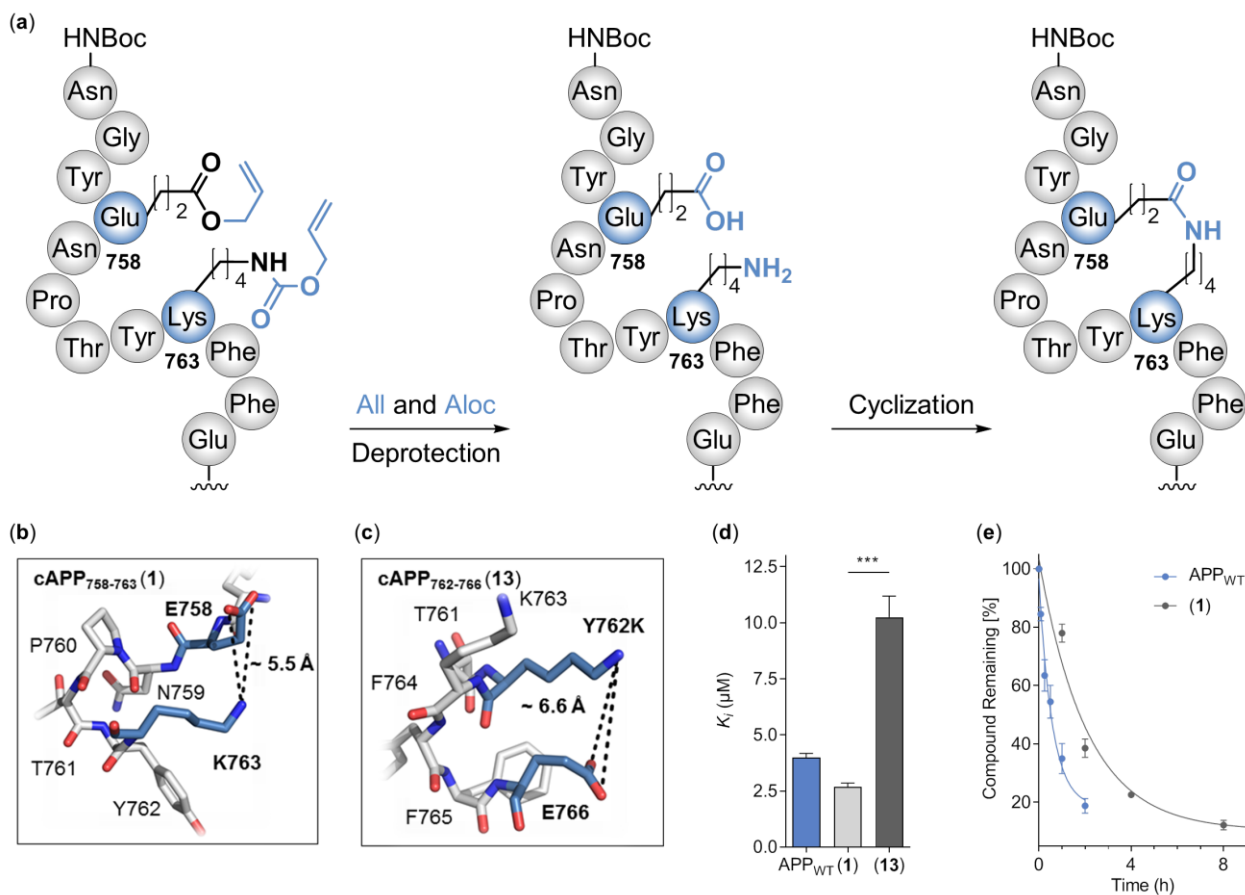


**Figure S12. Synthesis, structural feasibility, binding affinity and metabolic stability of cyclic APP<sub>WT</sub> variants.** (a) On-resin synthesis of cyclic APP<sub>WT</sub> through assembly of the linear precursor, followed by deprotection of All and Aloc protecting groups using (Pd(PPh<sub>3</sub>)<sub>4</sub>) - 0.2 eq. and PhSiH<sub>3</sub> - 20 eq. in dry DCM (1 mL), 2x15 min) and on-resin cyclization (PyBOP - 2.0 eq. and DIPEA - 2.0 eq. in DMF (1 mL)). (b) Stick representation of the APP ligand with residues E758 and K763 or (c) residues Y762K and E766 used for cyclization highlighted in blue yielding cAPP<sub>758-763</sub> (**1**) and cAPP<sub>762-766</sub> (**13**), respectively; (PDB ID: 3SV1).<sup>11</sup> (d)  $K_i$  values of APP<sub>WT</sub>, cAPP<sub>758-763</sub> (**1**) and cAPP<sub>Y762K-E766</sub> (**13**); data expressed as mean + SEM (n = 3), statistical significance was evaluated using one-way ANOVA with Dunnett's multiple comparison test, \*\*\* P<0.001. (e) Plasma stability of the APP<sub>WT</sub> peptide compared to cyclic analogue **1**; data expressed as mean + SEM (n = 3).

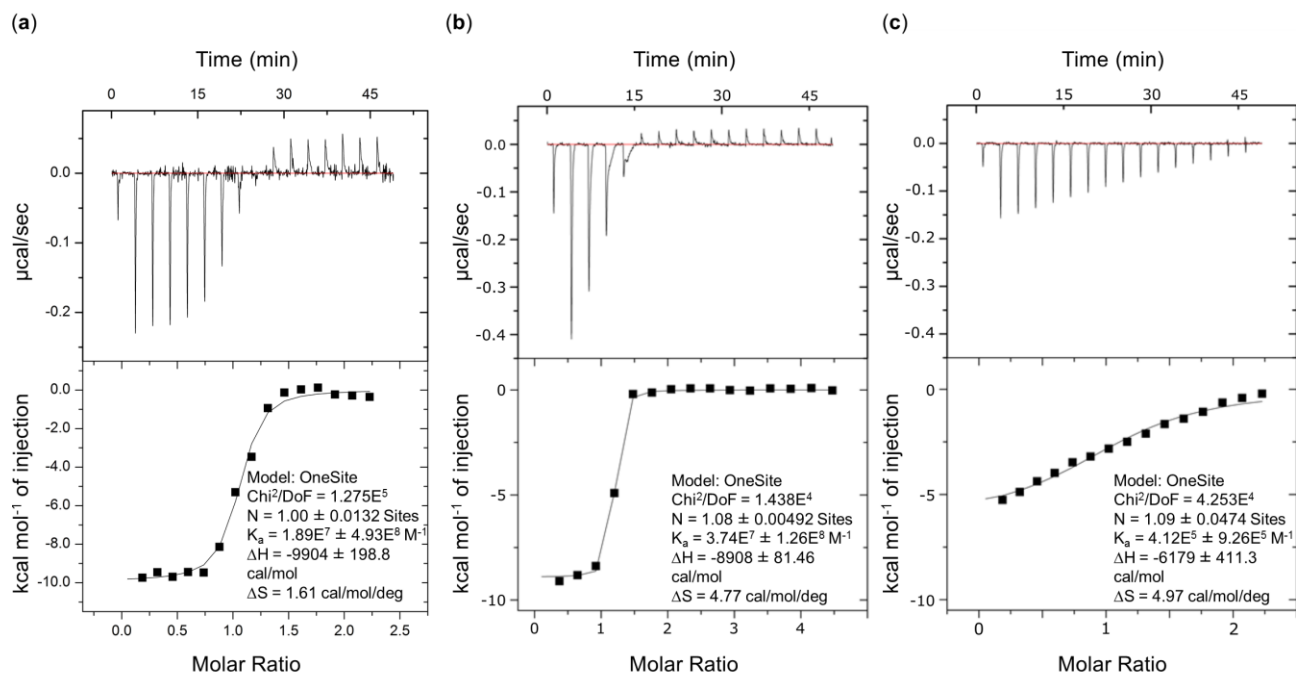


**Figure S13. ITC spectra of KSL-221036 (14, a and b) and the APP<sub>WT</sub> peptide (c).** Raw heat signatures (top) and integrated molar heat release including measurement specific parameters (bottom) obtained from titrating peptides with recombinant Mint2-PARM protein. (a) Titration of peptide 14 with Mint2-PARM:  $K_d = 53 \pm 2$  nM, (b) Titration of peptide 14 with Mint2-PARM:  $K_d = 30 \pm 8$  nM, (c) Titration of the APP<sub>WT</sub> peptide with Mint2-PARM:  $K_d = 2.4$   $\mu\text{M}$ .

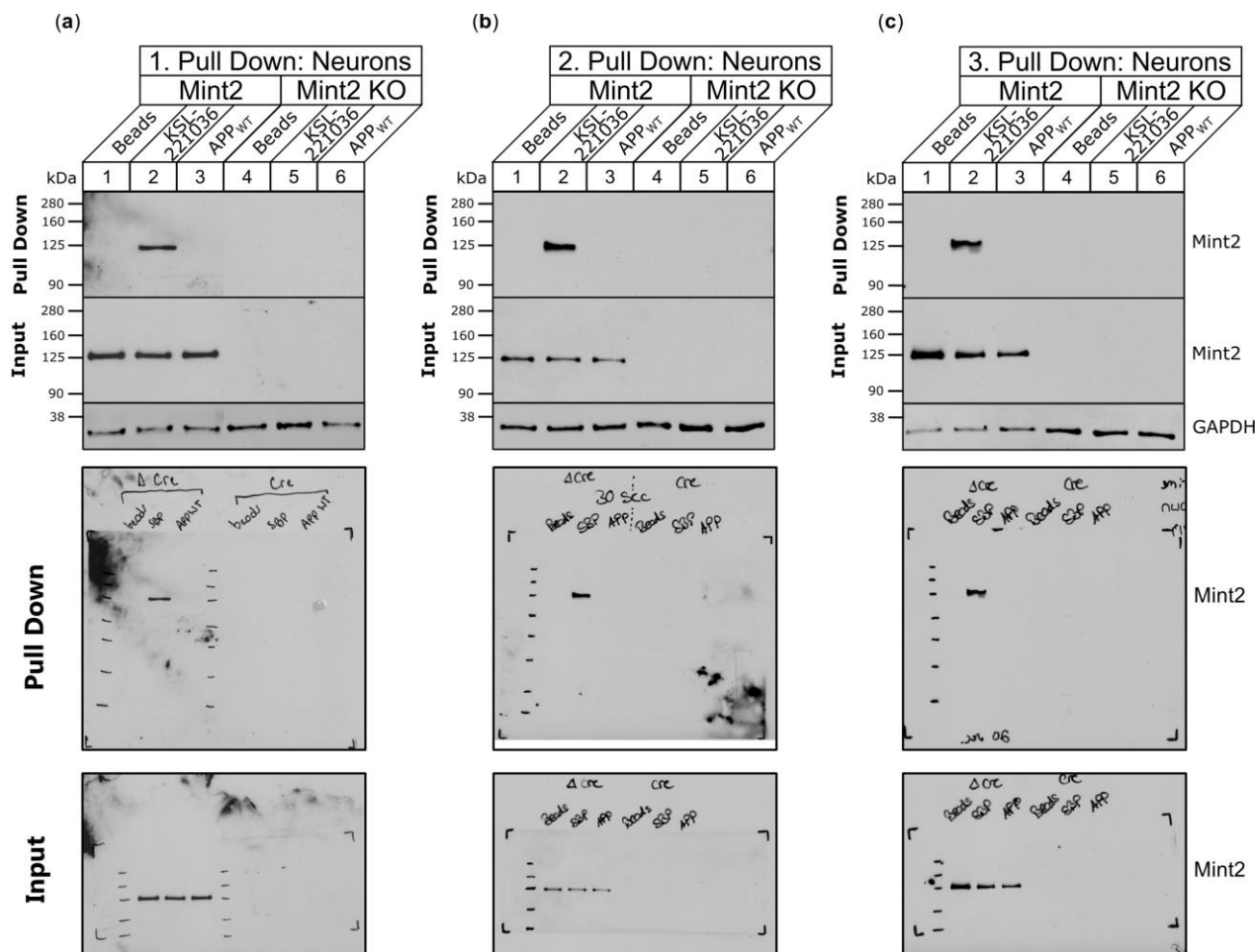


**Figure S14. Pull down of full length Mint2 using coated bead containing KSL-221036 (14) and APP<sub>WT</sub>.** Pull down of Mint2 from neuronal cell lysate collected 15 DIV (3 individual replicates; a to c). Pull down (b) was used to generate Figure 5c in the article. Neurons were cultured from Mint1 and 3 knockout mice with floxed Mint2 alleles. Pull down from cell lysate of neurons expressing Mint2 (input, lanes 1–3; original pictures  $\Delta cre$ ) is compared to pull down from neurons treated with active *cre* recombinase resulting in Mint2 knockout (input, lanes 4–6; original pictures *cre*). Immobilized KSL-221036 (14) pulled down more Mint2 (pull down, lanes 2) compared to immobilized APP<sub>WT</sub> (pull down, lanes 3). Neuronal lysates resolved by SDS-PAGE and immunoblotted for Mint2 and GAPDH (loading control). Corresponding original pictures (pull down and input) of developed western blot films using ECL Prime (30 sec incubation) are shown below. For peptides utilized see Table S1.

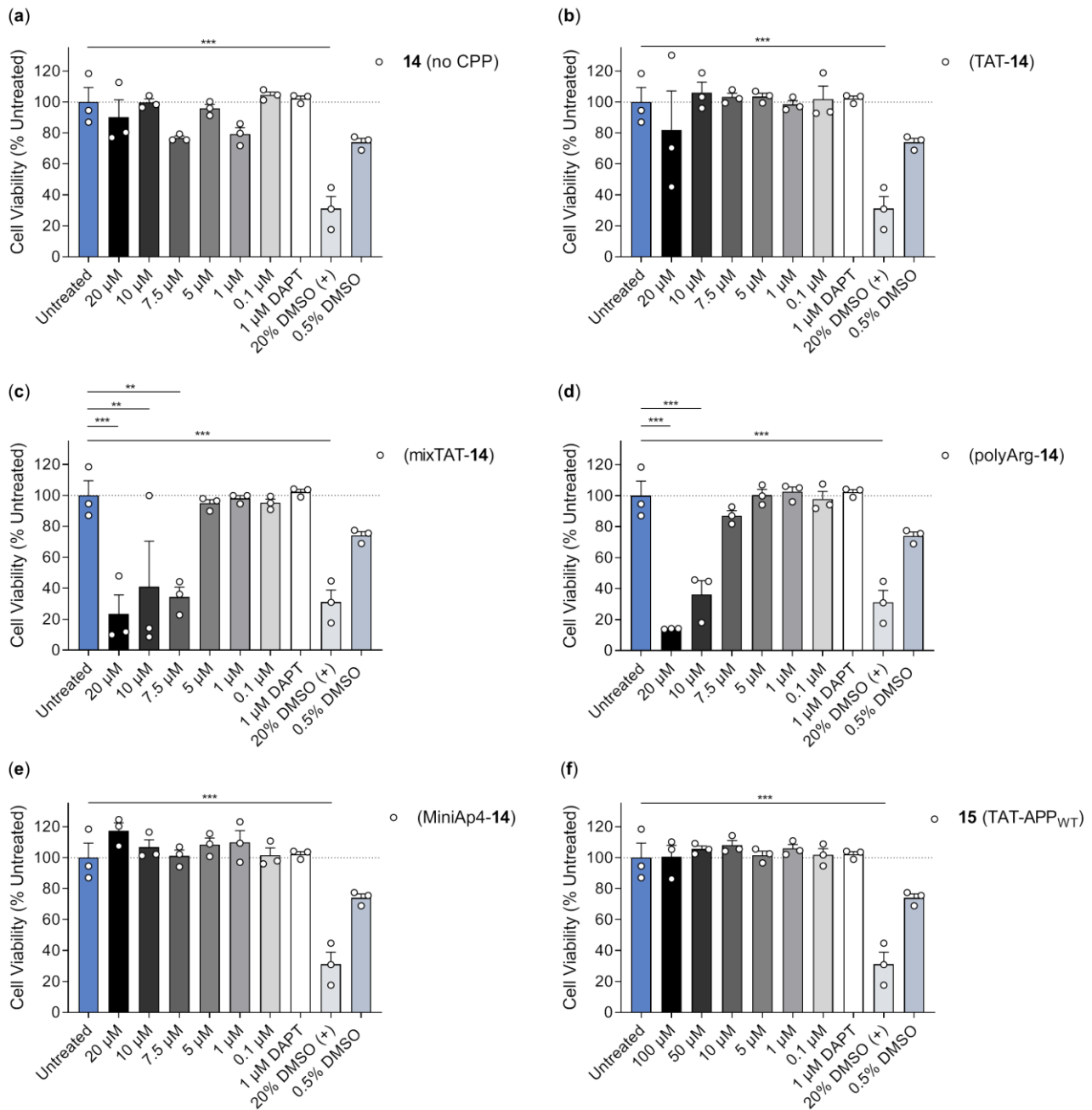


**Figure S15. Cytotoxicity of peptides.** Primary neurons from transgenic mice carrying the APP<sup>swe</sup>/PS1 $\Delta$ E9 transgene (7 DIV) were incubated with increasing concentrations of: (a) **14** (KSL-221036, no CPP); (b) (TAT<sup>47-57</sup>-**14**); (c) (mixTAT-**14**); (d) (polyArg-**14**); (e) (MiniAp4-**14**); and (f) **15** (TAT<sup>47-57</sup>-APP<sub>WT</sub>) for 24 h. Data expressed as % viability normalized to untreated neurons (untreated; same reference used for all peptides) and shown as individual points mean + SEM (n = 3 biological replicates), statistical significance was evaluated against vehicle using one-way ANOVA with Dunnett's multiple comparison test, \*\* P < 0.01, \*\*\* P < 0.001.

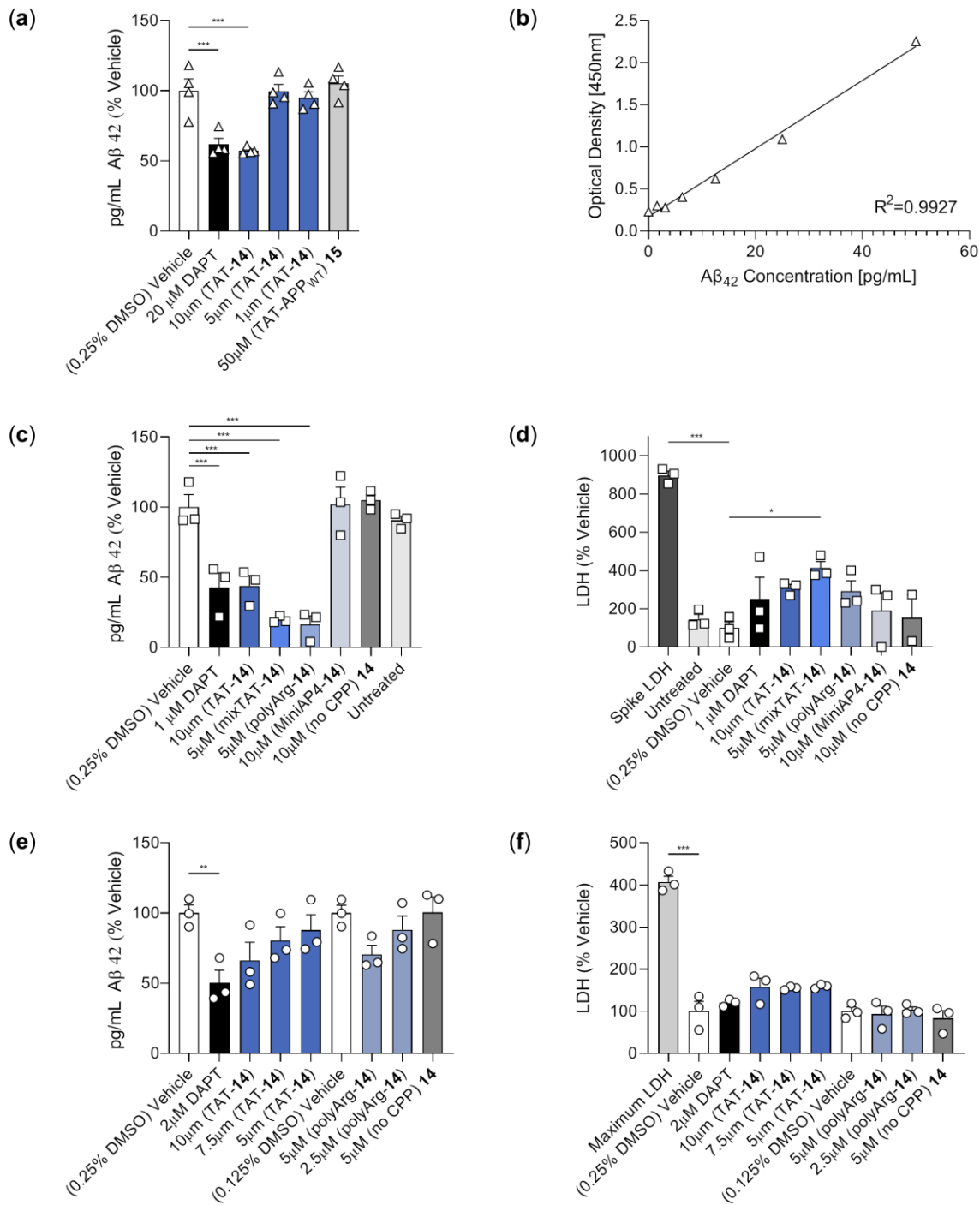


**Figure S16. Aβ<sub>42</sub> ELISA data and corresponding LDH data for each individual experiment.** Panels a, c, e: Normalized pg/mL Aβ<sub>42</sub> (vehicle = 100%) from the ELISA assay performed on conditioned medium of cultured neurons overproducing Aβ incubated with peptides for 24h. Data shown as individual points as well as mean + SEM (n = 3/4 biological replicates). Panel b: Representative Aβ<sub>42</sub> standard curves used to convert optical density to pg/mL Aβ<sub>42</sub> in panel (a). Panels (d, f): LDH levels in conditioned medium of cultured neurons overproducing Aβ incubated with peptides for 24h. Data expressed as % LDH normalized to vehicle control (and shown as individual points mean + SEM). Statistical significance for both the ELISA and LDH were evaluated using one-way ANOVA combined with either Dunnett's multiple comparison test (ELISA) or Sidak's multiple comparison test (LDH), \* P<0.05, \*\* P<0.01, \*\*\* P<0.001. First assay (a, b), second assay (c, d), third assay (e, f). Shapes for each individual data point are consistent with the shapes for each data point utilized in Figure 5f, g.

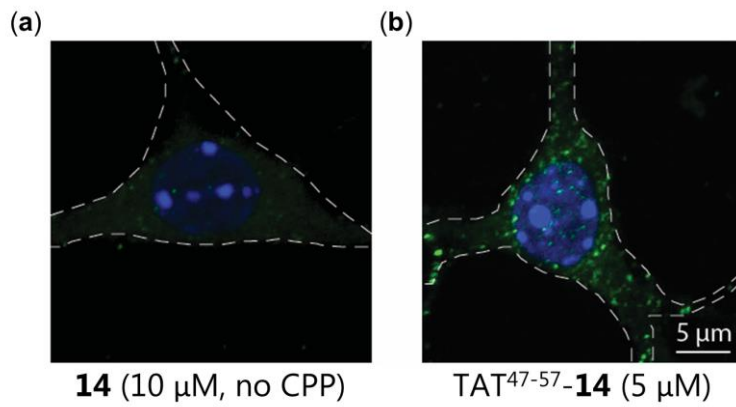


**Figure S17. Representative Z-stack images of TAT-immunostaining.** At 7 DIV primary hippocampal neurons from transgenic mice carrying the APP<sup>swE</sup>/PS1 $\Delta$ E9 transgene were incubated with (a) **14** (10  $\mu$ M, no CPP) or (b) **TAT<sup>47-57</sup>-14** (5  $\mu$ M) for 24 h. TAT immunoreactivity (green) and DAPI nuclear staining (blue) are shown, white dashed lines outline the cell body.



**Table S1. Characterization and affinities of APP peptides.**

APP Peptide	Sequence	Purity (%)	Calculated mass [M+H <sup>+</sup> ]	Observed mass [M+H <sup>+</sup> ]	K <sub>i</sub> (μM)	
TAMRA-APP <sub>C-term</sub>	(TAMRA) –NNG– 754QNGYENPTYKFFEQMQN770	> 95	2836.0	2835.3	n.d.	
minimal binding sequence	(754-770)	754QNGYENPTYKFFEQMQN770	> 90	2138.3	2137.4	2.9 ± 0.3
	(755-770)	755NGYENPTYKFFEQMQN770	> 95	2010.2	2009.2	4.2 ± 0.4
	(756-770)	756GYENPTYKFFEQMQN770	> 95	1896.1	1895.2	37.7 ± 3.8
	(757-770)	757YENPTYKFFEQMQN770	> 95	1839.0	1838.2	582 ± 87
	(754-769)	754QNGYENPTYKFFEQMQ769	> 95	2024.2	2023.2	4.9 ± 0.9
	(754-768)	754QNGYENPTYKFFEQM768	> 95	1896.0	1895.2	5.6 ± 0.5
	(754-767)	754QNGYENPTYKFFEQ767	> 95	1764.9	1764.2	6.5 ± 0.7
	(754-766)	754QNGYENPTYKFFE766	> 95	1636.7	1636.8	7.2 ± 0.8
	(754-765)	754QNGYENPTYKFF765	> 95	1507.6	1507.0	30.2 ± 0.9
	(754-764)	754QNGYENPTYKF764	> 95	1360.5	1360.0	329 ± 12
	(754-763)	754QNGYENPTYK763	> 95	1213.3	1212.6	635 ± 84
	APP <sub>WT</sub> (755-766)	755NGYENPTYKFFE766	> 95	1508.6	1508.6	4.0 ± 0.2
Ala-scan	N755A	755AGYENPTYKFFE766	> 95	1466.5	1465.6	1.6 ± 0.2
	G756A	755NAGYENPTYKFFE766	> 95	1523.6	1523.6	11.9 ± 1.3
	Y757A	755NGAENPTYKFFE766	> 95	1417.5	1416.6	305 ± 16
	E758A	755NGYANPTYKFFE766	> 95	1451.5	1451.7	12.2 ± 1.2
	N759A	755NGYEAPTYKFFE766	> 95	1466.5	1465.6	811 ± 43
	P760A	755NGYENATYKFFE766	> 95	1483.5	1482.6	25.4 ± 2.3
	T761A	755NGYENPAYKFFE766	> 95	1479.5	1478.6	14.2 ± 1.3
	Y762A	755NGYENPTAKFFE766	> 95	1417.5	1416.6	9.3 ± 1.0
	K763A	755NGYENPTYAKFFE766	> 95	1452.5	1451.6	5.5 ± 0.4
	F764A	755NGYENPTYKAFE766	> 95	1433.5	1432.6	56.9 ± 4.4
	F765A	755NGYENPTYKFAE766	> 95	1433.5	1432.7	72.9 ± 7.7
E766A	755NGYENPTYKFFA766	> 95	1451.5	1450.6	5.4 ± 0.5	
A-to-E	G756γ	755NγYENPTYKFFE766	> 90	1509.7	1508.6	32.3 ± 1.3
	Y757ψ	755NGψENPTYKFFE766	> 90	1509.7	1509.6	454 ± 79
	E758ε	755NGYεNPTYKFFE766	> 95	1509.7	1509.6	13.6 ± 0.4
	N759ν	755NGYENνPTYKFFE766	> 95	1509.7	1509.6	22.8 ± 1.5
	F764φ	755NGYENPTYKφFE766	> 95	1509.7	1509.6	11.5 ± 1.2
L-to-D AA	N755n	755nGYENPTYKFFE766	> 95	1508.7	1508.8	5.1 ± 0.2
	Y757y	755NGyENPTYKFFE766	> 95	1508.7	1508.7	266 ± 30.6
	E758e	755NGYenPTYKFFE766	> 95	1508.7	1508.7	>500
	N759n	755NGYENnPTYKFFE766	> 95	1508.7	1508.7	>500
	P760p	755NGYENpTYKFFE766	> 95	1508.7	1508.6	>500
	T761t	755NGYENPtYKFFE766	> 95	1508.7	1508.7	170 ± 27.8
	Y762y	755NGYENPTYkFFE766	> 95	1508.7	1508.7	208 ± 1.5
	K763k	755NGYENPTYKfFFE766	> 95	1508.7	1508.7	89.4 ± 5.8
	F764f	755NGYENPTYKfFE766	> 95	1508.7	1508.7	79.7 ± 4,1
	F765f	755NGYENPTYKffE766	> 95	1508.7	1508.7	32.4 ± 2.5
	E766e	755NGYENPTYKFFE766	> 95	1508.7	1508.7	5.4 ± 0.7

TAMRA – 5/6-Carboxytetramethylrhodamine; K<sub>i</sub> data is presented as mean ± SEM, n = 3.

**Table S1. Characterization and affinities of APP peptides (continued).**

	APP Peptide	Sequence	Purity (%)	Calculated mass [M+H <sup>+</sup> ]	Observed mass [M+H <sup>+</sup> ]	K <sub>i</sub> (μM)
NMe-AA scan	N755NMe	<sup>755</sup> N (Me) GYENPTYKFFFE <sup>766</sup>	> 95	1522.7	1522.6	2.5 ± 0.1
	G756NMe	<sup>755</sup> NG (Me) YENPTYKFFFE <sup>766</sup>	> 95	1522.7	1522.7	4.7 ± 0.3
	Y757NMe	<sup>755</sup> NGY (Me) ENPTYKFFFE <sup>766</sup>	> 95	1522.7	1522.6	>500
	E758NMe	<sup>755</sup> NGYE (Me) NPTYKFFFE <sup>766</sup>	> 95	1522.7	1522.6	9.8 ± 0.7
	N759NMe	<sup>755</sup> NGYEN (Me) PTYKFFFE <sup>766</sup>	> 95	1522.7	1522.6	38.2 ± 8.2
	T761NMe	<sup>755</sup> NGYENPT (Me) YKFFFE <sup>766</sup>	> 95	1522.7	1522.7	44.8 ± 6.0
	Y762NMe	<sup>755</sup> NGYENPTY (Me) KFFFE <sup>766</sup>	> 95	1522.7	1522.6	51.1 ± 7.2
	K763NMe	<sup>755</sup> NGYENPTYK (Me) FFE <sup>766</sup>	> 95	1522.7	1522.6	81.8 ± 8.4
	F764NMe	<sup>755</sup> NGYENPTYKF (Me) FE <sup>766</sup>	> 95	1522.7	1522.6	55.2 ± 5.5
	F765NMe	<sup>755</sup> NGYENPTYKFF (Me) E <sup>766</sup>	> 95	1522.7	1522.6	59.6 ± 9.9
	E766NMe	<sup>755</sup> NGYENPTYKFFFE (Me) <sup>766</sup>	> 95	1522.7	1522.6	7.2 ± 0.2
	Structure Activity Relationship	Y757pY	<sup>755</sup> NGpYENPTYKFFFE <sup>766</sup>	> 95	1588.6	1588.6
Y757F		<sup>755</sup> NGFENPTYKFFFE <sup>766</sup>	> 95	1492.7	1492.7	5.1 ± 0.6
Y757Nal1		<sup>755</sup> NGNal1ENPTYKFFFE <sup>766</sup>	> 95	1543.7	1543.6	1.7 ± 0.2
N759Q		<sup>755</sup> NGYEQPTYKFFFE <sup>766</sup>	> 95	1522.7	1522.7	>500
N759D		<sup>755</sup> NGYEDPTYKFFFE <sup>766</sup>	> 95	1508.7	1508.6	>500
N759E		<sup>755</sup> NGYEEPTYKFFFE <sup>766</sup>	> 95	1522.7	1522.6	>500
N759Dap		<sup>755</sup> NGYEDapPTYKFFFE <sup>766</sup>	> 95	1480.7	1480.7	>500
N759Dab		<sup>755</sup> NGYEDabPTYKFFFE <sup>766</sup>	> 95	1494.7	1494.7	>500
N759Orn		<sup>755</sup> NGYEOrnPTYKFFFE <sup>766</sup>	> 95	1508.7	1508.7	>500
N7592Abu		<sup>755</sup> NGYE2AbuPTYKFFFE <sup>766</sup>	> 95	1497.7	1497.7	>500
N759Nva		<sup>755</sup> NGYENvaPTYKFFFE <sup>766</sup>	> 95	1493.7	1493.7	>500
Y762K		<sup>755</sup> NGYENPTKKFFFE <sup>766</sup>	> 95	1473.8	1473.7	>500
Y762W		<sup>755</sup> NGYENPTWKFFFE <sup>766</sup>	> 95	1531.7	1531.6	9.8 ± 0.9
Y762F		<sup>755</sup> NGYENPTFKFFFE <sup>766</sup>	> 95	1492.7	1492.6	1.0 ± 0.1
F764Nal1		<sup>755</sup> NGYENPTYKNal1FE <sup>766</sup>	> 95	1558.7	1558.7	1.5 ± 0.4
F764W		<sup>755</sup> NGYENPTYKWFE <sup>766</sup>	> 95	1547.7	1547.6	5.2 ± 0.3
F765Nal1		<sup>755</sup> NGYENPTYKFNa11E <sup>766</sup>	> 95	1558.7	1558.7	2.6 ± 0.5
F765W		<sup>755</sup> NGYENPTYKFE <sup>766</sup>	> 95	1547.7	1547.6	5.4 ± 0.7
F764Igl, F765Igl		<sup>755</sup> NGYENPTYKIglIglE <sup>766</sup>	> 95	1560.7	1560.6	6.0 ± 0.3
F764Nal2, F765Nal2		<sup>755</sup> NGYENPTYKNal2Na12E <sup>766</sup>	> 95	1608.7	1608.6	1.7 ± 0.1
F764Nal1, F765Nal1		<sup>755</sup> NGYENPTYKNal1Na11E <sup>766</sup>	> 95	1609.6	1609.6	1.1 ± 0.3

N(Me) indicates *N*-methylation of the amino acid; pY – L-phosphotyrosine; Non-proteinogenic amino acids are presented with three letter abbreviations: Nal1 – L-3-(1-naphthyl)alanine, Dap – L-2,4-diamino-propionic acid, Dab – L-2,4diaminobutyric acid, Orn – L-ornithine, Abu – L-2-aminobutyric acid, Nva – L-norvaline, Igl – 2-indanyl-L-glycine, Nal2 – L-3-(2-naphthyl)alanine; K<sub>i</sub> data is presented as mean ± SEM, n = 3.

**Table S1. Characterization and affinities of APP peptides** (continued)

APP Peptide	Sequence	Purity (%)	Calculated mass [M+H <sup>+</sup> ]	Observed mass [M+H <sup>+</sup> ]	K <sub>i</sub> (μM)	
cAPP <sup>E758-K763</sup> <b>1</b> n = 2, m = 4	<sup>755</sup> NGYc[ <b>ENPTYK</b> ]FFE <sup>766</sup>	> 95	1490.7	1490.7	2.7 ± 0.2	
cAPP <sup>Y762K-E766</sup> <b>2</b>	<sup>755</sup> NGYENPTc [ <b>KKFFE</b> ] <sup>766</sup>	> 95	1455.7	1455.6	10.3 ± 0.9	
Side chain-to-side chain lactam cyclization scan	<b>3</b> n = 1, m = 4	<sup>755</sup> NGYc[ <b>DNPTYK</b> ]FFE <sup>766</sup>	> 95	1476.7	1476.5	4.2 ± 0.4
	<b>4</b> n = 2, m = 3	<sup>755</sup> NGYc[ <b>ENPTYOrn</b> ]FFE <sup>766</sup>	> 95	1476.7	1476.6	4.4 ± 0.2
	<b>5</b> n = 1, m = 3	<sup>755</sup> NGYc[ <b>DNPTYOrn</b> ]FFE <sup>766</sup>	> 95	1462.6	1462.6	13.6 ± 0.9
	<b>6</b> n = 2, m = 2	<sup>755</sup> NGYc[ <b>ENPTYDap</b> ]FFE <sup>766</sup>	> 95	1462.6	1462.6	19.6 ± 1.0
	<b>7</b> n = 1, m = 2	<sup>755</sup> NGYc[ <b>DNPTYDap</b> ]FFE <sup>766</sup>	> 95	1448.6	1448.5	6.4 ± 0.5
	<b>8</b> n = 4, m = 2	<sup>755</sup> NGYc[ <b>KNPTYE</b> ]FFE <sup>766</sup>	> 95	1490.7	1490.6	2.4 ± 0.2
	<b>9</b> n = 3, m = 2	<sup>755</sup> NGYc[ <b>OrnNPTYE</b> ]FFE <sup>766</sup>	> 95	1476.7	1476.6	2.8 ± 0.4
	<b>10</b> n = 4, m = 1	<sup>755</sup> NGYc[ <b>KNPTYD</b> ]FFE <sup>766</sup>	> 95	1476.7	1476.6	2.2 ± 0.3
	<b>11</b> n = 2, m = 2	<sup>755</sup> NGYc[ <b>DapNPTYE</b> ]FFE <sup>766</sup>	> 95	1462.6	1462.6	35.0 ± 2.0
	<b>12</b> n = 3, m = 1	<sup>755</sup> NGYc[ <b>OrnNPTYD</b> ]FFE <sup>766</sup>	> 95	1462.6	1462.6	2.3 ± 0.1
	<b>13</b> n = 2, m = 1	<sup>755</sup> NGYc[ <b>DapNPTYD</b> ]FFE <sup>766</sup>	> 95	1448.6	1448.5	79.9 ± 1.4
	KSL-221036 <b>14</b>	<sup>755</sup> (NMea) GYc [KNPTYD] (Nall) (Nall) e <sup>766</sup>	> 95	1548.7	1548.6	30 ± 8 nM*
	Pull down	APP <sub>WT</sub> , PD	C (PEG2) – <sup>755</sup> NGYENPTYKFFE <sup>766</sup>	> 95	1757.9	1757.6
<b>14</b> -PD		C (PEG2) – KSL-221036	> 95	1797.0	1796.7	n.d.
CPP-tagged	TAT <sup>47-57</sup> - <b>14</b>	Ac-YGRKRRQRRR- <b>14</b>	> 90	1044.5 [M+3H] <sup>3+</sup>	1044.5 [M+3H] <sup>3+</sup>	n.d.
	mixTAT- <b>14</b>	Ac-rRrGrKkrK- <b>14</b>	> 90	469.4 [M+6H] <sup>6+</sup>	469.8 [M+6H] <sup>6+</sup>	n.d.
	polyArg- <b>14</b>	Ac-RRRRRRRRR- <b>14</b>	> 90	499.9 [M+6H] <sup>6+</sup>	500.2 [M+6H] <sup>6+</sup>	n.d.
	D-SynB3- <b>14</b>	Ac-frrrrsyslrr- <b>14</b>	> 95	742.6 [M+4H] <sup>4+</sup>	743.0 [M+4H] <sup>4+</sup>	n.d.
	MiniAp4- <b>14</b>	c (DLATEPAK (Dap) ) - <b>14</b>	> 95	1221.1 [M+2H] <sup>2+</sup>	1221.1 [M+2H] <sup>2+</sup>	n.d.
	<b>15</b> (TAT <sup>47-57</sup> -APP <sub>WT</sub> )	Ac-YGRKRRQRRR- <sup>755</sup> NGYENPTYKFFE <sup>766</sup>	> 95	1031.2 [M+3H] <sup>3+</sup>	1031.7 [M+3H] <sup>3+</sup>	n.d.

c[...] = side chain to side chain cyclized peptide; Nall – L-3-(1-naphthyl)alanine; \*K<sub>d</sub> value measured by ITC; n.d. = not determined; PD = pull down peptides; PEG = polyethylenglycole linker; Ac = N-terminal acetylated; K<sub>i</sub> data is presented as mean ± SEM, n = 3.

**Table S2. Characterization and affinities of PARM variants.**

(PARM 364-570)	Purity (%)	Calculated mass [M+H]	Observed mass [M+H]	$K_d$ ( $\mu$ M)
PARM-His6	> 95	25237	25237	12.0 $\pm$ 0.16
C483A, C501A, C566A	> 95	25141	25141	9.8 $\pm$ 0.30
R455K, C483A, C501A, C566A	> 95	25113	25112	13.0 $\pm$ 0.79
L454A	> 95	25195	25193	139 $\pm$ 1.5
L454E	> 90	25253	25249	141 $\pm$ 3.7
L454K	> 95	25252	25250	114 $\pm$ 15
R455A	> 95	25152	25150	18.1 $\pm$ 0.63
T456A	> 95	25207	25206	27.6 $\pm$ 0.82
I457A	> 95	25195	25193	17.5 $\pm$ 0.44
S458A	> 95	25221	25220	3.0 $\pm$ 0.03
Y459A	> 95	25145	25143	180 $\pm$ 4.6
Y459E	> 90	25203	25200	195 $\pm$ 5.8
I460A	> 95	25195	25193	5.0 $\pm$ 0.08
D462A	> 95	25193	25192	6.1 $\pm$ 0.18
Q510A	> 95	25180	25178	20.9 $\pm$ 0.35
Q514A	> 95	25180	25178	7.0 $\pm$ 0.09
F520A	88	25161	25159	542 $\pm$ 6.8
F520E	> 95	25219	25219	127 $\pm$ 0.81
F520K	> 95	25219	25218	294 $\pm$ 18
Y524A	> 95	25145	25144	67.7 $\pm$ 2.2
F527A	> 90	25161	25160	43.6 $\pm$ 1.09
L454A, Y459A	> 95	25103	25101	203 $\pm$ 7.6
L454A, F520A	> 95	25119	25119	655 $\pm$ 18
Y459A, F520A	> 95	25069	25068	895 $\pm$ 43

$K_d$  data expressed as mean  $\pm$  SEM, n = 3.

**Table S3. Characterization of PARM peptide fragments.**

Peptide ( $\Delta_{\text{pep}}\text{PARM}$ )	Sequence (R = mercapto-acetyl-L-leucine)	Purity (%)	Calculated mass [M+H] <sup>+</sup>	Observed mass [M+H] <sup>+</sup>
WT	Thz-LKTISYIADIGNIVVLMARRRMPRS-R	> 95	3176.7	3176.0
R455 $\kappa$ <sup>1,2</sup>	Thz-L $\kappa$ TISYIADIGNIVVLMARRRMPRS-R	> 85	3177.7	3177.0
T456 $\tau$ <sup>2</sup>	Thz-LK $\tau$ ISYIADIGNIVVLMARRRMPRS-R	> 75	3177.7	3177.0
I457 $\iota$ <sup>1,2</sup>	Thz-LKT $\iota$ SYIADIGNIVVLMARRRMPRS-R	> 80	3177.7	3177.4
S458 $\sigma$ <sup>2</sup>	Thz-LKTI $\sigma$ YIADIGNIVVLMARRRMPRS-R	> 85	3177.7	3177.0
Y459 $\psi$	Thz-LKTIS $\psi$ IADIGNIVVLMARRRMPRS-R	> 75	3177.7	3177.0
I460 $\iota$	Thz-LKTISY $\iota$ ADIGNIVVLMARRRMPRS-R	> 80	3177.7	3176.9
A461 $\alpha$ <sup>2</sup>	Thz-LKTISYI $\alpha$ DIGNIVVLMARRRMPRS-R	> 75	3177.7	3177.0
D462 $\delta$	Thz-LKTISYIA $\delta$ IGNIVVLMARRRMPRS-R	> 75	3177.7	3177.0

<sup>1</sup>Building block strategy, <sup>2</sup>Oxidized methionine reduced after HF cleavage using a previously reported protocol.<sup>7</sup>

**Table S4. Characterization of semi synthetic Mint2-pPARMSS A-to-E variants and APPWT affinity.**

PARM 364-570 <sup>1</sup>	Purity (%)	Calculated mass	Observed mass	$K_d$ ( $\mu$ M)
		$[M+H]^+$	$[M+H]^+$	
pPARM <sub>ss</sub>	> 90	23410	23409	12.9 $\pm$ 0.4
R455 $\kappa$	> 90	23411	23409	38.5 $\pm$ 4.4
T456 $\tau$	> 90	23411	23409	22.3 $\pm$ 1.0
I457 $\iota$	> 95	23411	23409	55.8 $\pm$ 1.6
S458 $\sigma$	> 90	23411	23409	171 $\pm$ 6.3
Y459 $\psi$	> 90	23411	23409	29.0 $\pm$ 1.5
I460 $\theta$	> 90	23411	23409	36.6 $\pm$ 1.9
A461 $\alpha$	> 85	23411	23409	42.2 $\pm$ 1.9
D462 $\delta$	> 85	23411	23409	298 $\pm$ 13

<sup>1</sup>(R455K, C483A, C501A, C566A).  $K_d$  data for APP<sub>WT</sub> binding expressed as mean  $\pm$  SEM, n = 3.

### Supplementary References:

1. Stuhr-Hansen, N.; Padrah, S.; Strømgaard, K., Facile synthesis of  $\alpha$ -hydroxy carboxylic acids from the corresponding  $\alpha$ -amino acids. *Tetrahedron Lett.* **2014**, *55* (30), 4149-4151.
2. Deechongkit, S.; You, S.-L.; Kelly, J. W., Synthesis of all nineteen appropriately protected chiral  $\alpha$ -hydroxy acid equivalents of the  $\alpha$ -amino acids for Boc solid-phase depsi-peptide synthesis. *Org. Lett.* **2004**, *6* (4), 497-500.
3. Elgersma, R. C.; Meijneke, T.; Posthuma, G.; Rijkers, D. T. S.; Liskamp, R. M. J., Self-assembly of amylin(20–29) amide-bond derivatives into helical ribbons and peptide nanotubes rather than Fibrils. *Chem. Eur. J.* **2006**, *12* (14), 3714-3725.
4. Neises, B.; Steglich, W., Simple method for the esterification of carboxylic acids. *Angew. Chem. Int. Ed.* **1978**, *17* (7), 522-524.
5. Hang, J.; Li, H.; Deng, L., Development of a rapid, room-temperature dynamic kinetic resolution for efficient asymmetric synthesis of  $\alpha$ -aryl amino acids. *Org. Lett.* **2002**, *4* (19), 3321-3324.
6. Theile, C. S.; Witte, M. D.; Blom, A. E. M.; Kundrat, L.; Ploegh, H. L.; Guimaraes, C. P., Site-specific N-terminal labeling of proteins using sortase-mediated reactions. *Nat. Protoc.* **2013**, *8* (9), 1800-1807.
7. Hackenberger, C. P. R., The reduction of oxidized methionine residues in peptide thioesters with  $\text{NH}_4\text{I-Me}_2\text{S}$ . *Org. Biomol. Chem.* **2006**, *4* (11), 2291-2295.
8. Albertsen, L.; Shaw, A. C.; Norrild, J. C.; Strømgaard, K., Recombinant production of peptide C-terminal  $\alpha$ -amides using an engineered intein. *Bioconjug. Chem.* **2013**, *24* (11), 1883-1894.
9. Nikolovska-Coleska, Z.; Wang, R.; Fang, X.; Pan, H.; Tomita, Y.; Li, P.; Roller, P. P.; Krajewski, K.; Saito, N. G.; Stuckey, J. A., Development and optimization of a binding assay for the XIAP BIR3 domain using fluorescence polarization. *Anal. Biochem.* **2004**, *332* (2), 261-273.
10. Ho, A.; Morishita, W.; Atasoy, D.; Liu, X.; Tabuchi, K.; Hammer, R. E.; Malenka, R. C.; Sudhof, T. C., Genetic analysis of Mint/X11 proteins: Essential presynaptic functions of a neuronal adaptor protein family. *J. Neurosci.* **2006**, *26* (50), 13089-13101.